

# Zfp207 is a Bub3 binding protein regulating meiotic chromosome alignment in mouse oocytes

XiaoXin Dai<sup>1,\*</sup>, Hao Xiong<sup>2,\*</sup>, Mianqun Zhang<sup>1,\*</sup>, Shaochen Sun<sup>1</sup> and Bo Xiong<sup>1</sup>

<sup>1</sup> College of Animal Science and Technology, Nanjing Agricultural University, Nanjing, China

<sup>2</sup> The First Clinical Medical College, School of Medicine, Nanchang University, Nanchang, China

\* These authors have contributed equally to this work

Correspondence to: Bo Xiong, email: xiongbo@njau.edu.cn

Keywords: oocyte meiosis, Zfp207, chromosome alignment, K-MT attachment, aneuploid eggs, Pathology Section

Received: March 25, 2016

Accepted: May 01, 2016

Published: May 11, 2016

## ABSTRACT

Zinc finger proteins are a massive, diverse family of proteins that serve a wide variety of biological functions. However, the roles of them during meiosis are not yet clearly defined. Here, we report that Zfp207 localizes at the kinetochores during mouse oocyte meiotic maturation. Depletion of Zfp207 leads to a significantly higher proportion of impaired spindle organization and misaligned chromosomes in oocytes. This is coupled with the defective kinetochore-microtubule attachments, and resultantly increasing incidence of aneuploid metaphase II eggs. The precocious polar body extrusion and escape of metaphase I arrest induced by nocodazole treatment in Zfp207-depleted oocytes indicates that Zfp207 is essential for activation of SAC (Spindle Assembly Checkpoint) activity. Notably, we find that Zfp207 binds to Bub3 to form a complex and maintains its protein level in oocytes, and that overexpression of Bub3 is able to partially rescue the occurrence of aneuploid eggs in Zfp207-depleted oocytes. Collectively, we identify Zfp207 as a novel Bub3 binding protein in oocytes which plays an important role in controlling meiotic chromosome alignment and SAC function.

## INTRODUCTION

High-fidelity chromosome segregation ensures proper distribution of genetic material during cell division in both mitosis and meiosis [1]. Segregation errors during mitosis in somatic cells contribute to the development and progression of cancer, and segregation errors during meiosis in germ cells lead directly to miscarriages, birth defects and genetic disorders [2, 3]. To achieve faithful chromosome segregation, eukaryotic cells develop a high-fidelity surveillance system referred to as SAC (spindle assembly checkpoint) to prevent chromosome missegregation and aneuploidy by delaying anaphase onset until all kinetochores are successfully attached to the spindle microtubules with the proper tension at the metaphase plate [4-8].

SAC is mainly composed of the members of Bub and Mad families. Among them Mad2, BubR1 and Bub3 comprise the soluble Mitotic Checkpoint Complex (MCC)

which inhibits the activation of anaphase-promoting complex/cyclosome (APC/C) by targeting APC/C's cofactor Cdc20, and delays the metaphase-anaphase transition until correct kinetochore-microtubule attachment is established [3, 9, 10]. Once chromosome is properly aligned at metaphase plate with appropriate tension by the spindle, SAC pathway is shut down and Cdc20 is released to activate APC/C, which then ubiquitinates Securin and Cyclin B, leading to the activation of Separase to remove the Cohesin complex from chromosome and onset of anaphase [9, 11, 12].

Chromosome segregation during cell division is facilitated by the kinetochores. When microtubules are not bound, they prevent cell cycle progression by generating the SAC signal. The kinetochore, assembled from more than 90 proteins at the centromere, is a large multiprotein structure that is often divided up into three layers: inner, central, and outer [13, 14]. The inner proteins are associated with the DNA and are linked to the outer layer

by the central layer, and the outer kinetochore proteins are responsible for capturing microtubules and recruiting SAC components [7, 15-19]. Bub1, BubR1 and Bub3 are three core SAC proteins that are required for correct chromosome alignment and kinetochore-microtubule attachment. They form two heterodimers 'Bub1-Bub3' and 'BubR1-Bub3' at the kinetochores to exert the function [8, 20]. Bub3 recruits Bub1 and BubR1 by directly binding to a highly conserved GLEBS domain in Bub1 or BubR1 [8, 21, 22].

BuGZ (Bub3-interacting GLEBS-motif-containing ZNF207) /Znf207/Zfp207 is a zinc finger protein that also contains a GLEBS motif [16]. Recent studies have shown that BuGZ uses its GLEBS domain directly binds to and stabilizes Bub3 during interphase and mitosis [11, 14, 16]. As a Bub3-binding partner and chaperone, BuGZ promotes kinetochore-microtubule interaction, chromosome alignment, and mitotic progression in cancer cells [11] [14, 16]. Although it has been identified as a novel regulator of chromosome alignment in mitotic cells, its accurate role in meiosis has not yet been defined.

In the present study we provide a body of evidence demonstrating that Zfp207 is required for normal spindle organization, correct chromosome alignment, proper kinetochore-microtubule attachment, and maintenance of euploidy during mouse oocyte meiotic maturation. We also find that Zfp207 is implicated in promoting these events through, at least partially, regulation of Bub3.

## RESULTS

### Zfp207 localizes at the kinetochores in mouse oocytes

To examine the localization of Zfp207 during meiotic maturation in mouse oocytes, we tried several commercially available antibodies to perform the immunofluorescent analysis, but all of them were not working in oocytes. Therefore we made a construct to fuse the fluorescent tag mCherry to the C-terminus of Zfp207 and *in vitro* transcribed it into cRNA. The result of cRNA microinjection showed that Zfp207-mCherry was present at the end of chromosomes from GVBD till late metaphase I stage (Figure 1A). This localization pattern is quite similar to that of kinetochore proteins, thus we immunostained Zfp207-mCherry expressing oocytes with kinetochore marker Crest, and they indeed exhibited the overlapping fluorescent signals in the oocytes (Figure 1B), indicating that Zfp207 is localized at the kinetochores during meiosis.

### Zfp207 modulates meiotic spindle assembly and chromosome alignment in oocytes

The kinetochore localization of Zfp207 prompted us to examine its possible function in spindle organization and chromosome alignment. We then employed a morpholino-based gene-silencing approach to deplete Zfp207. Fully-grown GV oocytes were microinjected with control and Zfp207-specific morpholinos and arrested in medium supplemented with milrinone for 20 h, allowing enough time to deplete the endogenous Zfp207. Following arrest, the oocytes were washed in milrinone-free medium and cultured to metaphase I stage to analyze the spindle morphology and chromosome alignment. Oocytes were immunostained with anti-tubulin-FITC antibody to visualize the spindles and counterstained with PI for the chromosomes. The staining results showed that a large majority of oocytes exhibited a typical barrel-shape spindle and a well-aligned chromosome on the equatorial plate in the control MO-injected group (Figure 2A). In striking contrast, various types of aberrant spindle morphologies including elongated, shortened, multipolar and collapsed spindles as well as misaligned chromosomes were observed in Zfp207 MO-injected oocytes (Figure 2A). More than 45% of oocytes displayed the disorganized spindles and about 40% of oocytes exhibited misaligned chromosomes compared to less than 10% of defects in controls which might be caused by physical damage of microinjection and milrinone toxicity (Figure 2B, 2C). To rule out the possibility that defective spindle assembly and chromosome alignment was due to the off-target effects of morpholinos, we expressed the Zfp207-mCherry in Zfp207-depleted oocytes by injecting Zfp207-mCherry cRNA, and then observed the morphology of spindles and chromosomes. As expected, in the rescue oocytes, the rates of defective spindles and chromosomes were decreased to the levels that were comparable to controls (Figure 2B, 2C). Thus, the results suggest that Zfp207 is important for spindle assembly and chromosome alignment during mouse oocyte meiotic maturation.

Then we asked whether misalignment of chromosomes would produce aneuploidy, an incorrect number of chromosomes in mouse eggs, which might lead to miscarriage, embryonic lethality or genetic disorders. For this purpose, we analyzed the karyotype of metaphase II oocytes by chromosome spreading. As shown in Figure 3A, the number of single chromosomes (univalents) in the normal oocytes was 20, which is the prerequisite for genomic integrity. Whereas a much higher frequency of aneuploid eggs that had more or less 20 univalents occurred in Zfp207-depleted oocytes in comparison with control and rescue oocytes (Figure 3B).

Taken together, these findings suggest that loss of Zfp207 in oocytes are unable to properly assemble the spindles and align the chromosomes and thus prone to produce aneuploid eggs.

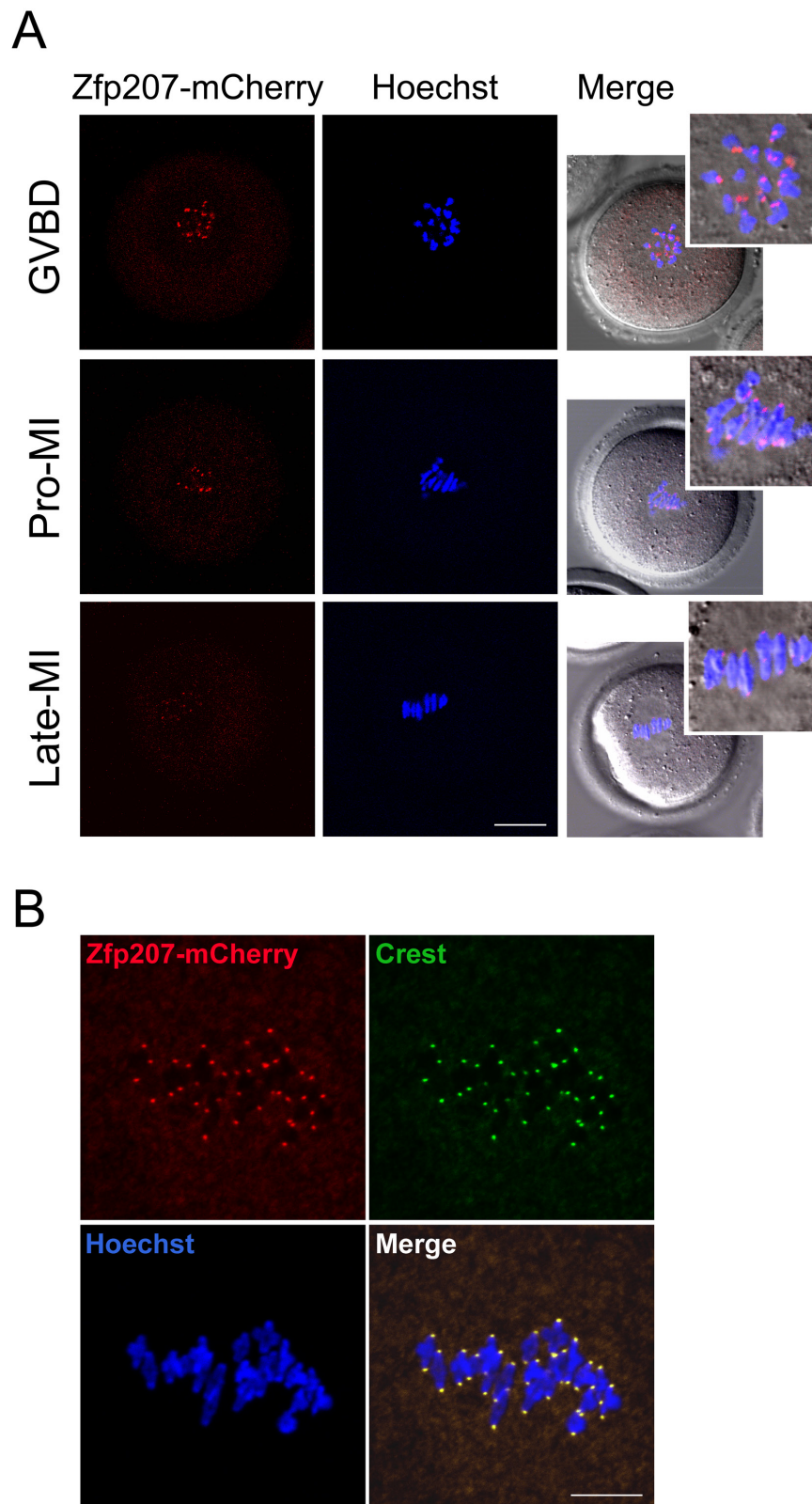


**Figure 1: Localization of Zfp207 during mouse meiotic maturation.** **A.** cRNA of Zfp207-mCherry was microinjected into GV oocytes which were then cultured to various developmental stages. mCherry signals were acquired under the confocal microscope at 594 nm laser. Chromosomes were counterstained with Hoechst. GVBD, oocytes at germinal vesicle breakdown stage; Pro-MI, oocytes at first prometaphase stage; Late-MI, oocytes at late stage of first metaphase. Scale bar, 20 $\mu$ m. **B.** Zfp207-mCherry expressing oocytes were immunostained with kinetochore marker Crest and then counterstained with Hoechst. Scale bar, 5 $\mu$ m.

## Zfp207 regulates kinetochore-microtubule attachment in oocytes

To determine whether the misalignment of chromosomes upon depletion of Zfp207 was caused by the defective interaction between kinetochores and microtubules, we assessed the stability of kinetochore-microtubule attachment by using cold treatment to depolymerize unstable microtubules that are not attached to kinetochores. To this end, metaphase I oocytes were briefly chilled at 4°C to induce depolymerization of unstable microtubules, and then immunostained with Crest to detect kinetochores, with anti-tubulin-FITC antibody to visualize the spindles and counterstained with Hoechst 33342 for chromosomes. We found that kinetochores became fully attached, chromosomes were well-aligned,

and spindles persisted after cold treatment in most of control MO-injected oocytes (Figure 4A, 4B). By contrast, in Zfp207-depleted oocytes, a significantly increased rate of kinetochores with very few cold-stable microtubules was observed compared to controls (Figure 4A, 4B). Whereas in the rescue oocytes expressing Zfp207-mCherry after depletion, the frequency of disrupted kinetochore-microtubule attachment was reduced to the rate comparable to controls (Figure 4B). Collectively, kinetochore-microtubule attachment forms less stably after depletion of Zfp207, which might contribute to the failure of chromosome alignment.

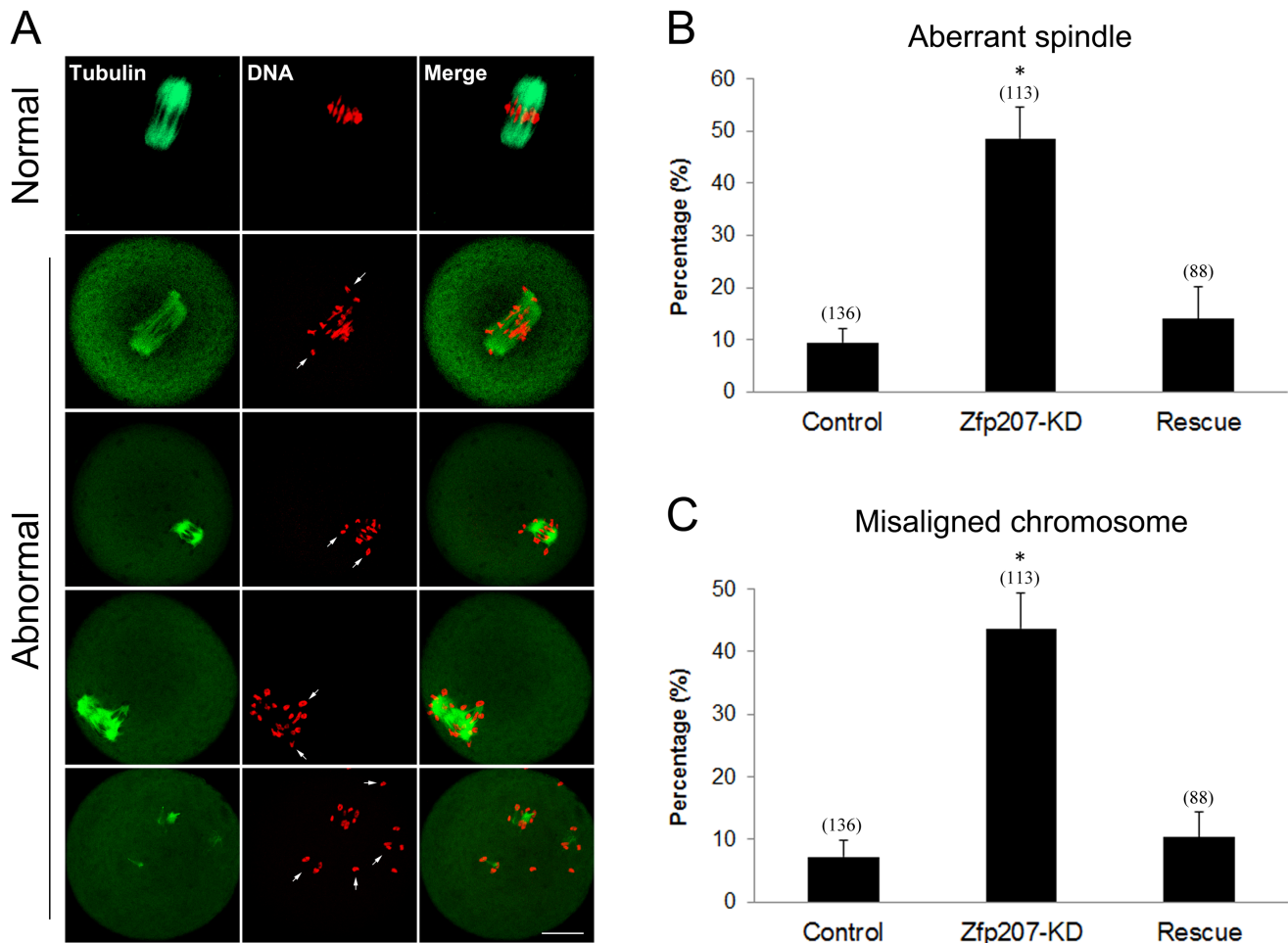


**Figure 2: Depletion of Zfp207 impairs spindle formation and chromosome alignment in mouse oocytes.** **A.** Representative images of normal and abnormal spindle morphologies and chromosome alignment in mouse oocytes. Oocytes were immunostained with  $\alpha$ -tubulin-FITC antibody to visualize spindle and counterstained with PI to visualize chromosome. Scale bar, 20 $\mu$ m. **B.** The rate of aberrant spindles was recorded in the control, Zfp207-KD and rescue oocytes. **C.** The rate of misaligned chromosomes was recorded in the control, Zfp207-KD and rescue oocytes. Data were presented as mean percentage (mean  $\pm$  SEM) of at least three independent experiments. Asterisk denotes statistical difference at a  $p < 0.05$  level of significance.

## Depletion of Zfp207 leads to premature polar body extrusion

Because we have already observed the defective spindle organization, chromosome alignment and kinetochore-microtubule attachment when depleted of Zfp207, we further investigated its possible effects on the oocyte meiotic progression. After culture of GV oocytes to the specific time points, the rates of GVBD and polar body extrusion were calculated in the control, Zfp207-depleted and Zfp207-rescue oocytes, respectively. We found that loss of Zfp207 did not affect either germinal vesicle breakdown or extrusion of first polar body (Figure 5A, 5B), two critical developmental events during oocyte maturation. However, at the time point of 7 h post-GVBD,

a higher incidence of PBE was observed in Zfp207-depleted oocytes compared to control and rescue oocytes (Figure 5C), suggesting that PBE occurred earlier in the absence of Zfp207.

The precocious PBE implied that SAC activity was compromised in Zfp207-depleted oocytes. To further confirm this possibility, we tested whether oocytes depleted of Zfp207 would abrogate the metaphase I arrest induced by nocodazole treatment, indicative of SAC inactivation. To this end, GV oocytes were cultured in medium supplemented with 0.04  $\mu\text{g/ml}$  of nocodazole for 12 h to observe the polar body extrusion. The result showed that only about 8% of control and 12% of rescue oocytes could override MI arrest and extrude the first polar body after 12 h of culture. While Zfp207-depleted oocytes displayed a remarkably increased overriding incidence

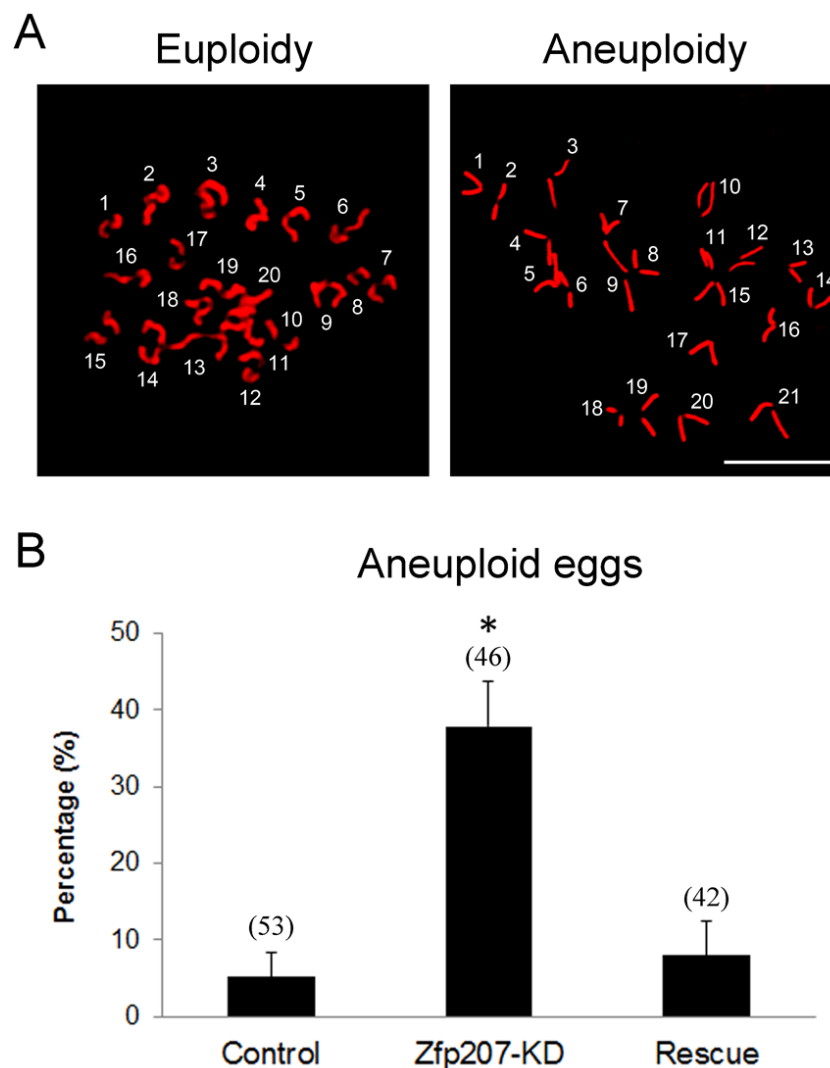


**Figure 3: Depletion of Zfp207 generates aneuploid eggs.** **A.** Representative images of euploid and aneuploid MII eggs. Chromosome spread was performed to calculate the number of chromosomes. Chromosomes were counterstained with PI. Scale bar, 5 $\mu\text{m}$ . **B.** The rate of aneuploid eggs was recorded in the control, Zfp207-KD and rescue oocytes. Data were presented as mean percentage (mean  $\pm$  SEM) of at least three independent experiments. Asterisk denotes statistical difference at a  $p < 0.05$  level of significance.

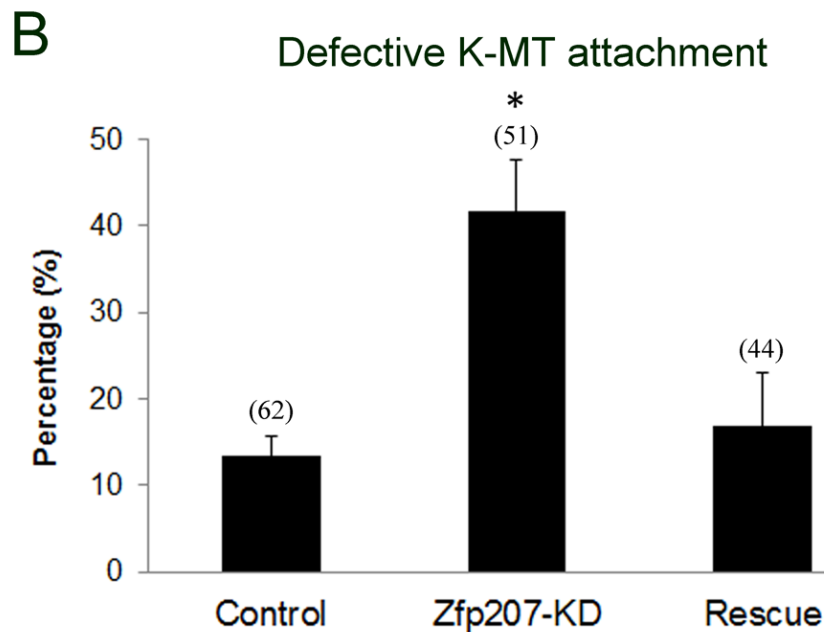
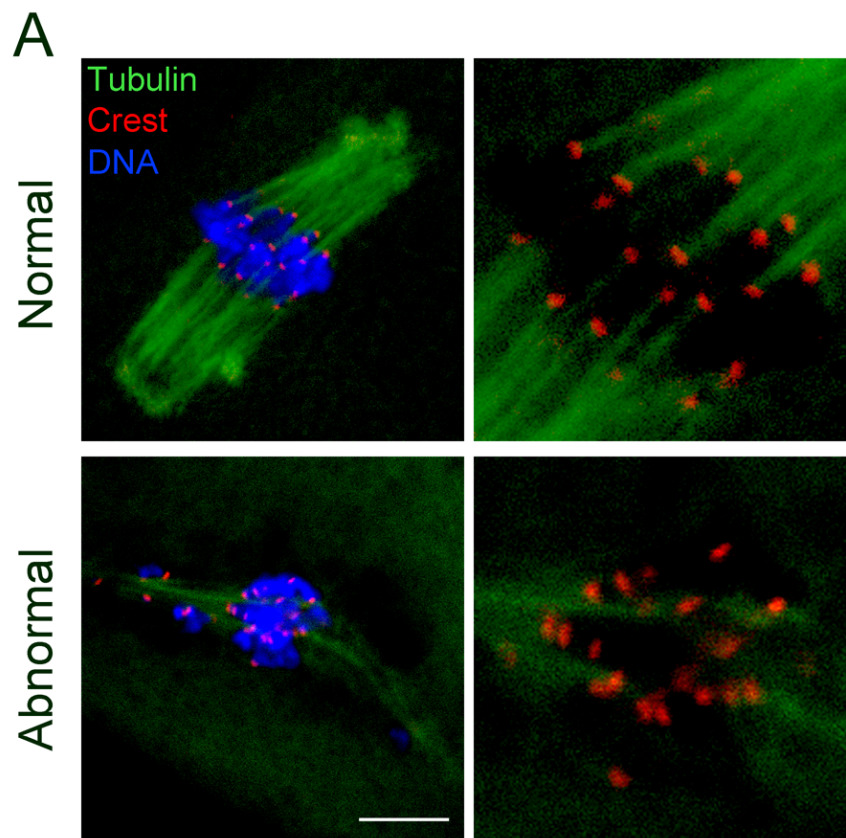


**Figure 4: Depletion of Zfp207 disrupts kinetochore-microtubule attachment in mouse oocytes.** **A.** Representative images of normal and abnormal kinetochore-microtubule attachment in mouse oocytes. Oocytes were immunostained with  $\alpha$ -tubulin-FITC antibody to visualize spindle, with Crest to visualize kinetochores, and counterstained with Hoechst to visualize chromosome. Scale bar, 10 $\mu$ m. **B.** The rate of defective kinetochore-microtubule attachment was recorded in the control, Zfp207-KD and rescue oocytes. Data were presented as mean percentage (mean  $\pm$  SEM) of at least three independent experiments. Asterisk denotes statistical difference at a  $p < 0.05$  level of significance.

and around 48% of oocytes escaped the MI arrest to reach the MII stage. Taken together, the above results imply that Zfp207 is required for SAC activation and might regulate SAC proteins during meiosis.

### Zfp207 forms a complex with Bub3 and affects its protein level in oocytes

Since Zfp207 is probably involved in the regulation of SAC function during mouse oocyte meiotic maturation, we next examined the protein levels of several important SAC proteins in Zfp207 MO-injected oocytes by western blotting. The result showed that depletion of Zfp207 did not affect the protein levels of Mad2, Bub1 and BubR1, three vital components of SAC in meiosis, but indeed obviously reduced the protein level of Bub3 (Figure 6A), suggesting that Bub3 might be the downstream molecule that mediates the role Zfp207 in chromosome alignment.

Given that Zfp207 regulates Bub3 in oocytes, we then asked whether Zfp207 interacts with Bub3 as a complex. To address this question, we first performed the cRNA microinjection to detect the localization relationship between Zfp207-mCherry and Bub3-GFP. The overlapping signals of mCherry and GFP revealed that Zfp207 colocalizes with Bub3 at kinetochores (Figure 6B). Moreover, we carried out Co-IP using oocyte lysates with Bub3 antibody. The blot of IP eluate probed by Bub3 antibody showed that Bub3 was specifically present in the antibody group instead of IgG control group (Figure 6C), suggesting that the complex containing Bub3 was pulled down in the eluate. Meanwhile, the blot probed by Zfp207 antibody also showed that Zfp207 appeared only in antibody group (Figure 6C), indicating that Zfp207 form a complex with Bub3 in oocytes.

The higher frequency of aneuploid eggs and decreased protein level of Bub3 in Zfp207-depleted oocytes prompted us to examine their correlation. To this

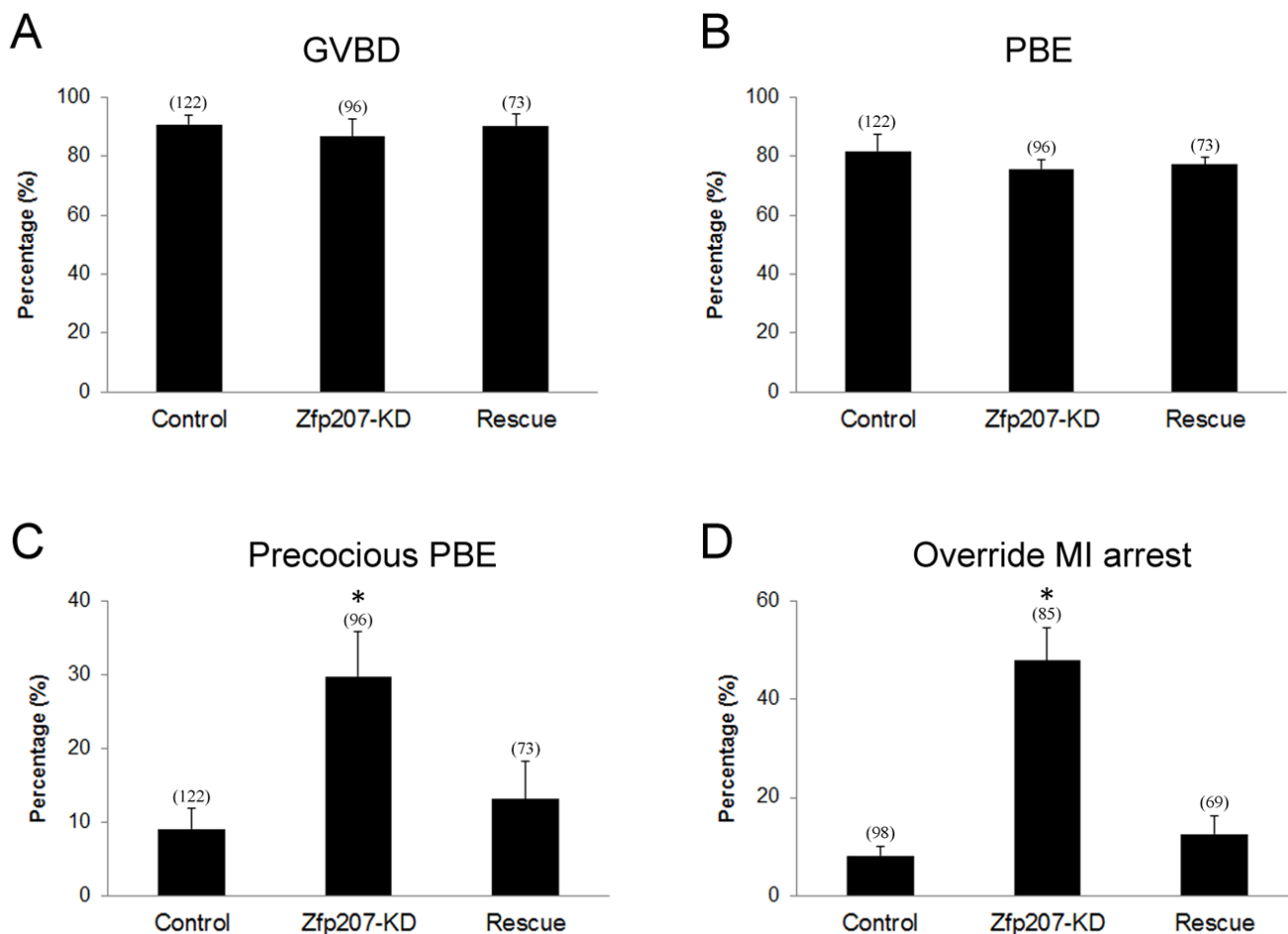


**Figure 5: Meiotic progression and SAC activation in Zfp207-depleted oocytes.** **A.** The rate of germinal vesicle breakdown was recorded in the control, Zfp207-KD and rescue oocytes. **B.** The rate of polar body extrusion was recorded in the control, Zfp207-KD and rescue oocytes. **C.** The rate of precocious polar body extrusion was recorded in the control, Zfp207-KD and rescue oocytes. **D.** The rate of overriding MI arrest was recorded in the control, Zfp207-KD and rescue oocytes. Data were presented as mean percentage (mean  $\pm$  SEM) of at least three independent experiments. Asterisk denotes statistical difference at a  $p < 0.05$  level of significance.

end, we co-expressed Bub3-GFP in Zfp207-MO injected oocytes and then observed the occurrence of aneuploidy. As shown in Figure 6D, overexpression of Bub3 could to a large extent rescue the phenotype of aneuploidy when depleted of Zfp207, confirming the fact that Bub3 works downstream of Zfp207.

## DISCUSSION

The highly conserved spindle assembly checkpoint mechanisms and components have been widely studied in mitosis, whereas the functional roles and components of SAC in meiosis are still not fully clear. Accumulated recent studies have shown that the SAC mechanism indeed operates in meiosis, and that many of its components are conserved between mitosis and meiosis [23, 24]. However, we currently do not know much about the

conserved differences between mitosis and meiosis, and even between the male and female meiosis in regulation of SAC [25].

Zinc finger proteins are among the most abundant proteins in eukaryotic genomes and participate in diverse biological events as interaction modules that bind DNA, RNA, proteins, or other small molecules [26, 27]. Recent studies in cancer cells have shown that BuGZ is a novel SAC component that is required for chromosome alignment *via* stabilizing Bub3 [11, 14, 16]. However, this mechanism does not work in normal somatic cells. The molecular basis of this selectivity is still an open question. Here, we report that Zfp207 plays a pivotal role in homologous chromosome segregation in mouse oocytes. Although we still cannot address the question why Zfp207 selectively exerts its functions in different cell lines, but our data provide first evidence showing that the function

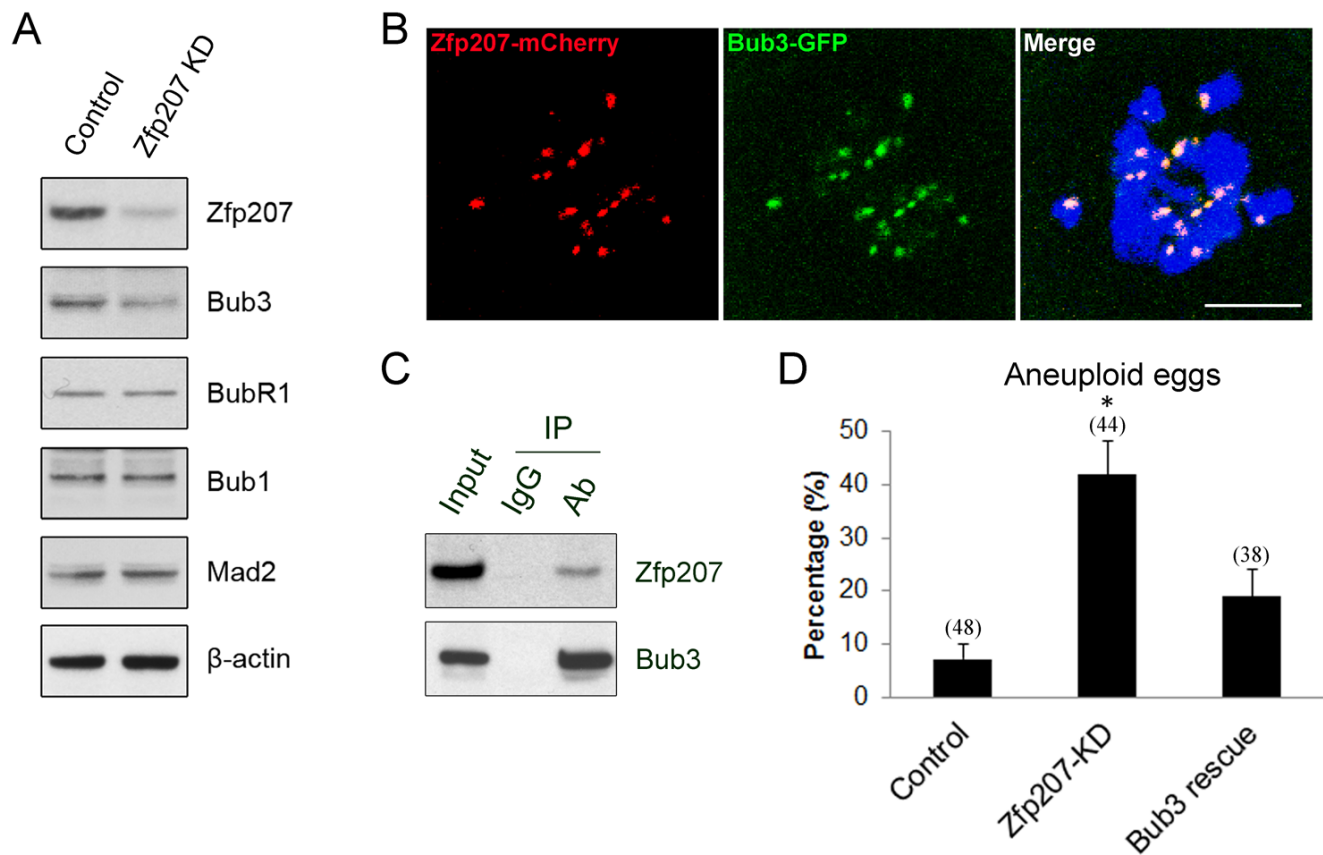


**Figure 6: Interaction between Zfp207 and Bub3 in mouse oocytes.** **A.** Protein levels of SAC components in Zfp207-knockdown oocytes were determined by western blotting. The blots of control and Zfp207-MO injected oocytes were probed with anti-Zfp207, anti-Bub3, anti-BubR1, anti-Bub1, anti-Mad2, and anti- $\beta$ -actin antibodies, respectively. **B.** Colocalization of Zfp207-mCherry and Bub3-GFP. GV oocytes were co-injected with cRNAs of Zfp207-mCherry and Bub3-GFP, and then cultured to Pro-MI stage. Signals of mCherry and GFP were acquired under confocal microscope at 594nm and 488nm laser, respectively. Chromosomes were counterstained with Hoechst. Scale bar, 5 $\mu$ m. **C.** Zfp207 associates with Bub3 in oocytes. Co-IP was performed to determine the interaction between Zfp207 and Bub3. Oocyte lysates were incubated with IgG and anti-Bub3 antibody, respectively, followed by incubation with protein G beads. The blots of IP eluates were probed with anti-Zfp207 and anti-Bub3 antibodies, respectively. **D.** Quantitative analysis of aneuploid eggs in the control, Zfp207-KD and Bub3-rescue oocytes. Data were presented as mean percentage (mean  $\pm$  SEM) of at least three independent experiments. Asterisk denotes statistical difference at a  $p < 0.05$  level of significance.

of Zfp207 in regulation of chromosome dynamics is conserved between mitosis and meiosis.

Consistent with the findings in cancer cells, our analyses show that Zfp207 localizes at kinetochores in oocytes after resumption of meiosis, and that depletion of Zfp207 by morpholino injection results in a higher incidence of aberrant spindle morphologies and misaligned chromosomes. These phenotypes are specific to the loss of Zfp207, because it can be rescued by the overexpression of Zfp207-mCherry. A large majority of incorrect chromosome alignment is usually caused by the impaired kinetochore-microtubule attachment, which is also exhibited in Zfp207-depleted oocytes. Our findings show that a significantly increased proportion of kinetochores are unattached by microtubules upon cool treatment which could depolymerize unattached microtubules. Since high-fidelity chromosome segregation prevents aneuploidy and maintains genome stability, our data also reveal that loss of Zfp207 produces a higher frequency of aneuploid eggs which are highly correlated with miscarriage, birth defects and genetic disorders.

Kinetochore-bound SAC proteins such as Mad1, Mad2, Bub1, BubR1, Bub3, and Mps1 generate the wait signal to give cells the time to align all chromosomes to the metaphase plate for equal chromosome segregation [9, 28, 29] [30]. Upon proper alignment of all chromosomes, the SAC signal has to be silenced for metaphase to anaphase transition. Our findings show that depletion of Zfp207 leads to the precocious poly body extrusion and escape of MI arrest induced by nocodazole treatment, two important features indicative of inactivation of SAC activity which have already been characterized in previous studies on SAC components such as Bub1, Bub3, BubR1 and Mad2 in mouse oocytes [3, 31-33]. The protein levels of these SAC components in the absence of Zfp207 have also been detected to figure out how Zfp207 affects SAC activity. In agreement with the observations in cancer cells, we find that protein level of Bub3 is markedly reduced upon knockdown of Zfp207, rather than that of Bub1, BubR1 and Mad2. This suggests that either Zfp207 regulates the protein expression of Bub3 or maintains the stability of Bub3 to ensure proper chromosome alignment in oocytes. Additionally, the colocalization and Co-IP analyses in our study show that Zfp207 binds to Bub3 to form a complex, which further confirms the interaction between Zfp207 and Bub3. Finally, overexpression of Bub3 is able to rescue the aneuploid phenotype of Zfp207-depleted oocytes, suggesting that the role of Zfp207 in regulation of chromosome alignment is, at least, partially mediated by Bub3.

Although several lines of evidence have been provided to demonstrate that Zfp207 is involved in chromosome alignment and activation of SAC during meiosis, many open questions still remain. For example, how does Zfp207 regulate Bub3's protein level in oocytes, through gene expression regulation or

protect it from degradation? Is there any other substrate working downstream of Zfp207? Is Zfp207 involved in chromosome segregation in early embryo development? A subsequent research needs to be done to clarify them.

## MATERIALS AND METHODS

### Antibodies

Rabbit polyclonal anti-Zfp207 antibody, sheep polyclonal anti-BubR1 antibody and mouse monoclonal anti-actin antibody were purchased from Abcam (Cambridge, MA, USA; Cat#: ab84802, ab28193 and ab3280); rabbit polyclonal anti-Bub3 antibody was purchased from Santa Cruz Biotechnology (Dallas, TX, USA; Cat#: sc-28258); mouse monoclonal anti- $\alpha$ -tubulin-fluorescein isothiocyanate (FITC) antibody and rabbit polyclonal anti-Bub1 antibody were purchased from Sigma (St. Louis, MO, USA; Cat#: F2168 and B3437); rabbit polyclonal anti-Mad2 antibody was purchased from Covance (Princeton, NJ, USA; Cat#: PRB-452C); Human anti-centromere CREST antibody was purchased from Antibodies Incorporated (Davis, CA, USA; Cat#: 15-234).

### Oocyte collection and culture

Animal care and use were conducted in accordance with the Animal Research Committee guidelines of Nanjing Agricultural University, China.

Female ICR mice (4-6 weeks) were sacrificed by cervical dislocation after intraperitoneal injections of 5 IU pregnant mare serum gonadotropin (PMSG) for 46 hours. Immature oocytes arrested at prophase of meiosis I were collected from ovaries in M2 medium (Sigma, St. Louis, MO, USA). Only those immature oocytes displaying a germinal vesicle (GV) were cultured further in M16 medium under liquid paraffin oil at 37°C in an atmosphere of 5% CO<sub>2</sub> in air. At different time points after culture, oocytes were collected for subsequent analysis.

### Morpholino knockdown and cRNA constructs

Fully grown GV-intact oocytes were microinjected with 5-10  $\mu$ l of non-targeting or Zfp207-targeting morpholinos (Gene tools, Philomath, OR, USA) in M2 medium containing 2.5  $\mu$ M milrinone. The working concentration of morpholinos was 1 mM. To facilitate the inhibition of mRNA translation by morpholinos, microinjected oocytes were arrested at GV stage in M16 medium containing 2.5  $\mu$ M milrinone for 20 h, and then transferred to milrinone-free M16 medium to resume the meiosis for further experiments. Zfp207 morpholino sequence: 5'-CTTCTTCTTGCGACCCATAACTGCG-3'.

Full-length of Zfp207 and Bub3 cDNAs were inserted into the pcDNA-3-EGFP vector (Addgene, Cambridge, MA, USA). Capped cRNAs were synthesized from linearized plasmid using T7 mMessage mMachine kit (ThermoFisher, Waltham, MA, USA), and purified with MEGAclean kit (ThermoFisher, Waltham, MA, USA). Typically, 10-12  $\mu$ l (4% of the oocyte volume) of 0.5-1.0  $\mu$ g/ $\mu$ l cRNA was injected into oocytes.

### Immunofluorescent and confocal microscopy

Oocytes were fixed in 4% paraformaldehyde in PBS (pH 7.4) for 30 minutes and permeabilized in 0.5% Triton-X-100 for 20 min at room temperature. Then, oocytes were blocked with 1% BSA-supplemented PBS for 1 h and incubated with 1:50-1:100 dilution of primary antibodies at 4°C overnight. After washing four times (5 min each) in PBS containing 1% Tween 20 and 0.01% Triton-X 100, oocytes were incubated with an appropriate secondary antibody for 1 h at room temperature. After washing three times, oocytes were counterstained with PI or Hoechst 33342 (10  $\mu$ g/ml) for 10 min. Finally, oocytes were mounted on glass slides and observed under a confocal laser scanning microscope (Carl Zeiss 700).

### Immunoprecipitation and immunoblotting analysis

Immunoprecipitation was carried out with rabbit polyclonal anti-Bub3 antibody according to the Instructions for ProFound Mammalian Co-Immunoprecipitation Kit (Pierce, Rockford, IL, USA).

For immunoblotting, oocytes were lysed in 4 $\times$  LDS sample buffer (ThermoFisher, Waltham, MA, USA) containing protease inhibitor and heated at 95°C for 5 min. Proteins were separated on 12% Bis-Tris precast gels, transferred to PVDF membranes, blocked in 5% nonfat milk in TBS (Tris buffered saline, pH 7.4) with 0.1% Tween 20 (TBST) for 1 h at room temperature, and then probed with 1:500 or 1:1000 dilution of primary antibodies at 4°C overnight. After washing three times in TBST (10 min each), blots were incubated 1 h with a 1:10,000 dilution of HRP (Horse Radish Peroxidase) conjugated secondary antibodies. Chemiluminescence was detected with ECL Plus (Pierce, Rockford, IL, USA) and signals were acquired by Tanon-3900.

### Chromosome spread

Oocytes were exposed to Tyrode's buffer (pH 2.5) for about 30 s at 37°C to remove zona pellucidae. After recovery in M2 medium for 10 min, oocytes were fixed in a drop of 1% paraformaldehyde with 0.15% Triton X-100 on a glass slide. After air drying, chromosomes

were counterstained with PI and examined under a laser scanning confocal microscope.

### Statistical analysis

The data were expressed as mean  $\pm$  SEM and analyzed by one-way ANOVA, followed by LSD's post hoc test, which was provided by SPSS16.0 statistical software. The level of significance was accepted as  $p < 0.05$ .

### ACKNOWLEDGMENTS

We thank Dr. Mo Li very much for providing plasmids.

### CONFLICTS OF INTEREST

The authors have no conflicts of interest to disclose.

### FUNDING

This work was supported by the National Natural Science Foundation (31571545) and Natural Science Foundation of Jiangsu Province (BK20150677).

### REFERENCES

1. Nicklas RB. How cells get the right chromosomes. *Science*. 1997; 275:632-637.
2. Compton DA. Spindle assembly in animal cells. *Annual review of biochemistry*. 2000; 69:95-114.
3. Wei L, Liang XW, Zhang QH, Li M, Yuan J, Li S, Sun SC, Ouyang YC, Schatten H and Sun QY. BubR1 is a spindle assembly checkpoint protein regulating meiotic cell cycle progression of mouse oocyte. *Cell cycle*. 2010; 9:1112-1121.
4. Hardwick KG. The spindle checkpoint. *Trends in genetics : TIG*. 1998; 14:1-4.
5. Jia L, Kim S and Yu H. Tracking spindle checkpoint signals from kinetochores to APC/C. *Trends in biochemical sciences*. 2013; 38:302-311.
6. Musacchio A and Hardwick KG. The spindle checkpoint: structural insights into dynamic signalling. *Nature reviews Molecular cell biology*. 2002; 3:731-741.
7. Huang H, Hittle J, Zappacosta F, Annan RS, Hershko A and Yen TJ. Phosphorylation sites in BubR1 that regulate kinetochore attachment, tension, and mitotic exit. *The Journal of cell biology*. 2008; 183:667-680.
8. Taylor SS, Ha E and McKeon F. The human homologue of Bub3 is required for kinetochore localization of Bub1 and a Mad3/Bub1-related protein kinase. *The Journal of cell biology*. 1998; 142:1-11.

9. Musacchio A and Salmon ED. The spindle-assembly checkpoint in space and time. *Nature reviews Molecular cell biology*. 2007; 8:379-393.
10. Cheeseman IM and Desai A. Molecular architecture of the kinetochore-microtubule interface. *Nature reviews Molecular cell biology*. 2008; 9:33-46.
11. Toledo CM, Herman JA, Olsen JB, Ding Y, Corrin P, Girard EJ, Olson JM, Emili A, DeLuca JG and Paddison PJ. BuGZ is required for Bub3 stability, Bub1 kinetochore function, and chromosome alignment. *Developmental cell*. 2014; 28:282-294.
12. Morrow CJ, Tighe A, Johnson VL, Scott MI, Ditchfield C and Taylor SS. Bub1 and aurora B cooperate to maintain BubR1-mediated inhibition of APC/CCdc20. *Journal of cell science*. 2005; 118:3639-3652.
13. Stukenberg PT and Burke DJ. Connecting the microtubule attachment status of each kinetochore to cell cycle arrest through the spindle assembly checkpoint. *Chromosoma*. 2015.
14. Jiang H, He X, Wang S, Jia J, Wan Y, Wang Y, Zeng R, Yates J, 3rd, Zhu X and Zheng Y. A microtubule-associated zinc finger protein, BuGZ, regulates mitotic chromosome alignment by ensuring Bub3 stability and kinetochore targeting. *Developmental cell*. 2014; 28:268-281.
15. Logarinho E, Resende T, Torres C and Bousbaa H. The human spindle assembly checkpoint protein Bub3 is required for the establishment of efficient kinetochore-microtubule attachments. *Molecular biology of the cell*. 2008; 19:1798-1813.
16. Ji Z and Yu H. A protective chaperone for the kinetochore adaptor Bub3. *Developmental cell*. 2014; 28:223-224.
17. Lara-Gonzalez P, Westhorpe FG and Taylor SS. The spindle assembly checkpoint. *Current biology : CB*. 2012; 22:R966-980.
18. Meraldi P and Sorger PK. A dual role for Bub1 in the spindle checkpoint and chromosome congression. *The EMBO journal*. 2005; 24:1621-1633.
19. Elowe S. Bub1 and BubR1: at the interface between chromosome attachment and the spindle checkpoint. *Molecular and cellular biology*. 2011; 31:3085-3093.
20. Millband DN and Hardwick KG. Fission yeast Mad3p is required for Mad2p to inhibit the anaphase-promoting complex and localizes to kinetochores in a Bub1p-, Bub3p-, and Mph1p-dependent manner. *Molecular and cellular biology*. 2002; 22:2728-2742.
21. Bailer SM, Siniossoglou S, Podtelejnikov A, Hellwig A, Mann M and Hurt E. Nup116p and nup100p are interchangeable through a conserved motif which constitutes a docking site for the mRNA transport factor gle2p. *The EMBO journal*. 1998; 17:1107-1119.
22. Wang X, Babu JR, Harden JM, Jablonski SA, Gazi MH, Lingle WL, de Groen PC, Yen TJ and van Deursen JM. The mitotic checkpoint protein hBUB3 and the mRNA export factor hRAE1 interact with GLE2p-binding sequence (GLEBS)-containing proteins. *The Journal of biological chemistry*. 2001; 276:26559-26567.
23. Niaux T, Hached K, Sotillo R, Sorger PK, Maro B, Benzra R and Wassmann K. Changing Mad2 levels affects chromosome segregation and spindle assembly checkpoint control in female mouse meiosis I. *PloS one*. 2007; 2:e1165.
24. Malmanche N, Maia A and Sunkel CE. The spindle assembly checkpoint: preventing chromosome mis-segregation during mitosis and meiosis. *FEBS letters*. 2006; 580:2888-2895.
25. Morelli MA and Cohen PE. Not all germ cells are created equal: aspects of sexual dimorphism in mammalian meiosis. *Reproduction*. 2005; 130:761-781.
26. Laity JH, Lee BM and Wright PE. Zinc finger proteins: new insights into structural and functional diversity. *Current opinion in structural biology*. 2001; 11:39-46.
27. Klug A. The discovery of zinc fingers and their applications in gene regulation and genome manipulation. *Annual review of biochemistry*. 2010; 79:213-231.
28. Kim S and Yu H. Mutual regulation between the spindle checkpoint and APC/C. *Seminars in cell & developmental biology*. 2011; 22:551-558.
29. Fang X and Zhang P. Aneuploidy and tumorigenesis. *Seminars in cell & developmental biology*. 2011; 22:595-601.
30. Musacchio A. Spindle assembly checkpoint: the third decade. *Philosophical transactions of the Royal Society of London Series B, Biological sciences*. 2011; 366:3595-3604.
31. Zhang D, Ma W, Li YH, Hou Y, Li SW, Meng XQ, Sun XF, Sun QY and Wang WH. Intra-oocyte localization of MAD2 and its relationship with kinetochores, microtubules, and chromosomes in rat oocytes during meiosis. *Biology of reproduction*. 2004; 71:740-748.
32. Yin S, Wang Q, Liu JH, Ai JS, Liang CG, Hou Y, Chen DY, Schatten H and Sun QY. Bub1 prevents chromosome misalignment and precocious anaphase during mouse oocyte meiosis. *Cell cycle*. 2006; 5:2130-2137.
33. Li M, Li S, Yuan J, Wang ZB, Sun SC, Schatten H and Sun QY. Bub3 is a spindle assembly checkpoint protein regulating chromosome segregation during mouse oocyte meiosis. *PloS one*. 2009; 4:e7701.

RESEARCH ARTICLE

# Melamine Impairs Female Fertility via Suppressing Protein Level of Juno in Mouse Eggs

Xiaoxin Dai, Mianqun Zhang, Yajuan Lu, Yilong Miao, Changyin Zhou, Shaochen Sun, Bo Xiong\*

College of Animal Science and Technology, Nanjing Agricultural University, Nanjing, 20095, China

\* [xiongbo@njau.edu.cn](mailto:xiongbo@njau.edu.cn)



OPEN ACCESS

**Citation:** Dai X, Zhang M, Lu Y, Miao Y, Zhou C, Sun S, et al. (2015) Melamine Impairs Female Fertility via Suppressing Protein Level of Juno in Mouse Eggs. PLoS ONE 10(12): e0144248. doi:10.1371/journal.pone.0144248

**Editor:** Cheng-Guang Liang, Inner Mongolia University, CHINA

**Received:** October 10, 2015

**Accepted:** November 15, 2015

**Published:** December 3, 2015

**Copyright:** © 2015 Dai et al. This is an open access article distributed under the terms of the [Creative Commons Attribution License](https://creativecommons.org/licenses/by/4.0/), which permits unrestricted use, distribution, and reproduction in any medium, provided the original author and source are credited.

**Data Availability Statement:** All relevant data are within the paper.

**Funding:** This work was funded by BK20150677 ([www.jstdt.gov.cn](http://www.jstdt.gov.cn)), Natural Science Foundation of Jiangsu Province, to BX; and 31571545 ([www.nsf.gov.cn](http://www.nsf.gov.cn)), National Natural Science Foundation, to BX. The funders had no role in study design, data collection and analysis, decision to publish, or preparation of the manuscript.

**Competing Interests:** The authors have declared that no competing interests exist.

## Abstract

Melamine is an organic nitrogenous compound widely used as an industrial chemical, and it has been recently reported by us that melamine has a toxic effect on the female reproductive system in mice, and renders females subfertile; the molecular basis, however, has not been adequately assessed. In the present study, we explore the underlying mechanism regarding how melamine compromises fertility in the mouse. The data showed that melamine exposure significantly impaired the fertilization capability of the egg during *in vitro* fertilization. To further figure out the cause, we analyzed ovastacin localization and protein level, the sperm binding ability of zona pellucida, and ZP2 cleavage status in unfertilized eggs from melamine fed mice, and no obvious differences were found between control and treatment groups. However, the protein level of Juno on the egg plasma membrane in the high-dose feeding group indeed significantly decreased compared to the control group. Thus, these data suggest that melamine compromises female fertility via suppressing Juno protein level on the egg membrane.

## Introduction

Melamine (1,3,5-triazine-2,4,6-triamine, or C<sub>3</sub>H<sub>6</sub>N<sub>6</sub>) is a nitrogen heterocyclic triazine compound [1, 2] which has been widely used as an industrial chemical in many plastics, adhesives, glues, and laminated products such as plywood, cement, cleansers, fire-retardant paint, and more [2, 3]. Melamine developed as a chemical in the 1830s, and had varied and widespread legitimate uses. A food safety incident broke out in China in 2008 which was involved with milk and infant formula along with other food materials and components being adulterated with melamine had attracted much attention to the limited usage of melamine [2]. Accumulating evidence has revealed that long-term exposure to melamine could damage the reproductive systems in mammals, and lead to male infertility and fetal toxicity in the rat [4]. Also, previous report by us has shown that melamine feeding renders female mice subfertile [5].

Fertilization is a culminating event in mammals, involved in two haploid cells, the egg and the sperm. They meet in the female reproductive tract, interact, and finally fuse to become a

new, genetically distinct, diploid cell [6, 7]. Accomplishment of fertilization needs several sequential steps of gamete interaction: Capacitated sperm bind to the zona pellucida surrounding eggs, and then release acrosomal contents by exocytosis and penetrate the ZP. After that, acrosome-reacted sperm reach, bind to and fuse with the egg membrane to form fertilized egg [8]. ZP is a glycoproteinaceous translucent matrix that surrounds the mammalian eggs and embryos, and plays important roles during oogenesis, sperm-egg binding, fertilization and implantation [9–11]. This matrix of human is composed of four glycoproteins ZP1, ZP2, ZP3, and ZP4, whereas mouse ZP is composed of ZP1, ZP2 and ZP3 (ZP4 being a pseudogene) [9, 12]. In the supramolecular structure model, sperm-binding site is an N-terminal domain of ZP2 that depends on the cleavage status of ZP2 [9, 13]. Subsequent to sperm membrane fusion with oolemma, cleavage of ZP2 helps in prevention of polyspermy [14].

Ovastacin is a pioneer component of mammalian cortical granules which belongs to a member of the large astacin family of metalloendoproteases [15, 16]. This oocyte-specific protein is exocytosed from cortical granules triggered by fertilization and is responsible for post-fertilization ZP2 cleavage to block sperm binding and polyspermy. Thus, in ovastacin-deficient mice, albeit fertilization, sperm are still able to bind to zona pellucida surrounding embryos because ZP2 remains intact, which accordingly, renders ovastacin-deficient females subfertile due to the polyspermy [14]. In addition, fetuin-B has been recently identified as the inhibitor of ovastacin, and genetic ablation of fetuin-B causes premature ZP hardening and, consequently, female infertility [17, 18]. This result shows that premature cleavage of ZP2 can result in infertility in mice.

Glycophosphatidylinositol (GPI)-anchored receptors on the egg surface are essential for fertilization because sperm lacking them render eggs infertile [19, 20]. A breakthrough was made in 2014 when Gavin J. Wright's group identified folate receptor 4 (Folr4) as the Izumo1 receptor, displayed on the surface of egg they named this protein "Juno" after the Roman goddess of fertility and marriage [7]. Juno is expressed on the surface of oocyte, a GPI-anchored protein that is essential for female fertility. Juno-deficient mice are infertile because eggs lacking Juno cannot fuse with normal acrosome reacted sperm [6, 7].

Our most recent report indicates that melamine negatively affects female fertility in mice [5]. Here, we further explore the possible molecular basis at several levels during fertilization, and our data provide the evidence showing that melamine compromises female fertility via regulating the protein level of Juno, rendering eggs non-fusible with sperm.

## Materials and Methods

### Ethic statement

Our study was approved by the Animal Research Institute Committee of Nanjing Agricultural University, China, and all mice were handled in accordance with the Committee guidelines. Mice were housed in a temperature-controlled room with proper darkness-light cycles, fed with a regular diet, and maintained under the care of the Laboratory Animal Unit, Nanjing Agricultural University, China. The mice were euthanized by cervical dislocation.

### Animals and feeding treatment

The female 4-week-old ICR mice were housed in separate cages at controlled condition of temperature (20–23°C) and illumination (12h light-dark cycle), and had free access to food and water throughout the period of the study. After 1 week acclimation to the laboratory environment, mice were randomly assigned to 3 groups (n = 40), with an average body weight of 18 g and were each orally given 0, 10 or 50mg/kg/d of melamine dissolved in water for 8 weeks. The

animals were observed each three days, and there were no one ill or dead during administration.

### *In vitro* fertility

Cauda epididymides were lanced in a dish of human tubal fluid (HTF) medium (EMD Millipore, Billerica, MA) to release sperm, followed by being capacitated for 1 hr (37°C, 5% CO<sub>2</sub>) and added to ovulated eggs at a concentration of  $4 \times 10^5$ /ml sperm in 100 $\mu$ l HTF for 5 hr at 37°C, 5% CO<sub>2</sub>. The presence of two pronuclei was scored as successful fertilization.

### Immunofluorescent and confocal microscopy

Ovulated eggs were fixed in 4% paraformaldehyde in PBS (pH 7.4) for 30 minutes and permeabilized in 0.5% Triton-X-100 for 20 min at room temperature. Then, oocytes were blocked with 1% BSA-supplemented PBS for 1 h and incubated at 4°C overnight or at room temperature for 4 h with rat monoclonal anti-mouse folr4 antibody (1:100, BioLegend, CA) or rabbit polyclonal anti-mouse ovastacin antibody (1:100, obtained from Dr. Jurrien Dean). After washing four times (5 min each) in PBS containing 1% Tween 20 and 0.01% Triton-X 100, eggs were incubated with an appropriate secondary antibody for 1 h at room temperature. Alexa Fluor 555 donkey anti-rabbit IgG (H+L) was obtained from Invitrogen (Carlsbad, CA). After washing three times, eggs were stained with PI or Hoechst 33342 (10  $\mu$ g/ml) for 10 min. Finally, eggs were mounted on glass slides and viewed under a confocal laser scanning microscope (Carl Zeiss 700).

### Western blot analysis

Ovulated eggs or two-cell embryos were lysed in 4 $\times$  LDS sample buffer with 10 $\times$  reducing reagent (Life Technologies-Invitrogen) and heated at 100°C for 5 min. Proteins were separated on 12% Bis-Tris precast gels, transferred to PVDF membranes, blocked in 5% nonfat milk in TBS (Tris buffered saline, pH 7.4) with 0.1% Tween 20 (TBST) for 1 hr at room temperature, and then probed with 1:500 dilution of M2c.2 antibody (obtained from Dr. Jurrien Dean) at 4°C overnight. After washing three times in TBST (10 min each), blots were incubated 1 hr with a 1:10,000 dilution of HRP (Horse Radish Peroxidase) conjugated goat anti-rabbit IgG (Santa cruz, Texas). Chemiluminescence was performed with ECL Plus (Piercenet) and signals were acquired by Tanon-3900.

### Sperm binding assay

Caudal epididymal sperm were isolated from wild-type ICR mice and placed under oil (Sigma-Aldrich, MO) in HTF medium previously equilibrated with 5% CO<sub>2</sub> and capacitated by an additional 1 hr of incubation at 37°C. Sperm binding to ovulated eggs or two-cell embryos isolated from control and melamine-treated mice was observed using capacitated sperm and control two-cell embryos as a negative wash control. Samples were fixed in 4% PFA for 30 min, stained with Hoechst 33342. Bound sperm were quantified from z projections acquired by confocal microscopy, and results reflect the mean  $\pm$  S.E.M. from at least three independently obtained samples, each containing 10–12 mouse eggs/embryos.

### Statistical analysis

The data were expressed as mean  $\pm$  SEM and analyzed by one-way ANOVA, followed by LSD's post hoc test, which was provided by SPSS16.0 statistical software. The level of significance was accepted as  $p < 0.05$ .

## Results

### Melamine exposure compromises the *in vitro* fertilization

Melamine feeding model was set up by eight-week diet, and was classified into control (0mg/kg/d), low-dose (10mg/kg/d) and high-dose (50mg/kg/d) groups. To confirm the *in vivo* fertility result reported previously, eggs from three groups were collected and used for *in vitro* fertilization, respectively. As shown in Fig 1, the fertilization rate of low-dose group is comparable to that of control group ( $85.0 \pm 2.2\%$  VS  $81.9 \pm 1.4\%$ ), but the rate of how-dose group is significantly lower than and low dose (50mg/kg/d) group, the high dose (50mg/kg/d) group was significantly decreased ( $P < 0.01$ ). Because there was no obvious defect on the fertilization in low-dose group, we only compared control and high-dose groups in below experiments.

### Melamine does not result in mislocalization and premature exocytosis of ovastacin in eggs

To determine the possible reason causing the failure of fertilization, we first examined the localization and protein level of ovastacin, an oocyte-specific metalloprotease in the cortical

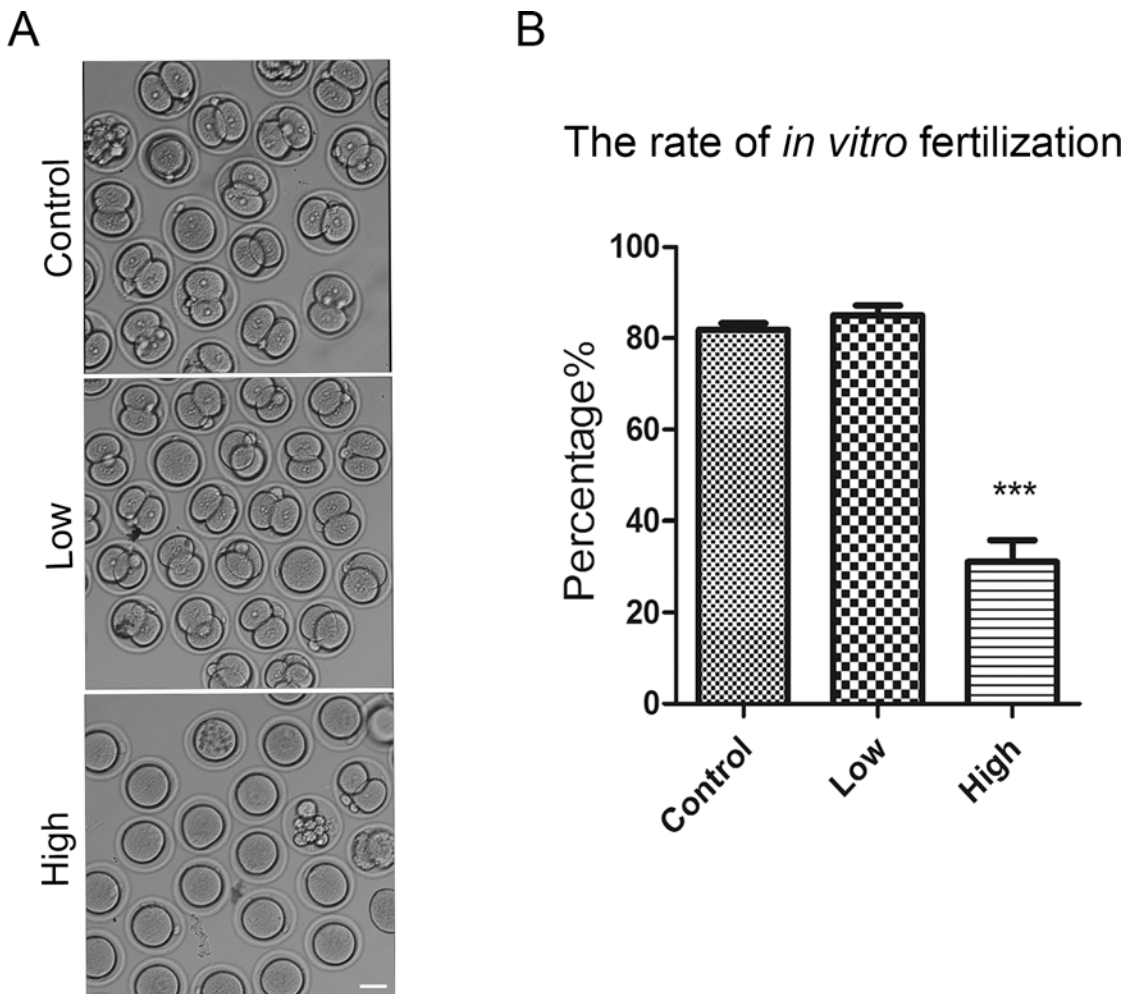


**Fig 1. *In vitro* fertilization of ovulated eggs from melamine fed mice.** (A) Representative images of fertilized eggs in control and melamine-treated mice. Most of eggs were not fertilized in high-dose treatment group. Scale bar, 40 $\mu$ m. (B) *In vitro* fertilization rates, control oocytes (n = 91), low group (n = 112), and high group (n = 124). Fertilization was determined by the presence of 2 pronuclei 12 hr after insemination. Data were presented as mean percentage (mean  $\pm$  SEM) of at least three independent experiments. Asterisk denotes statistical difference at a P < 0.05 level of significance.

doi:10.1371/journal.pone.0144248.g001

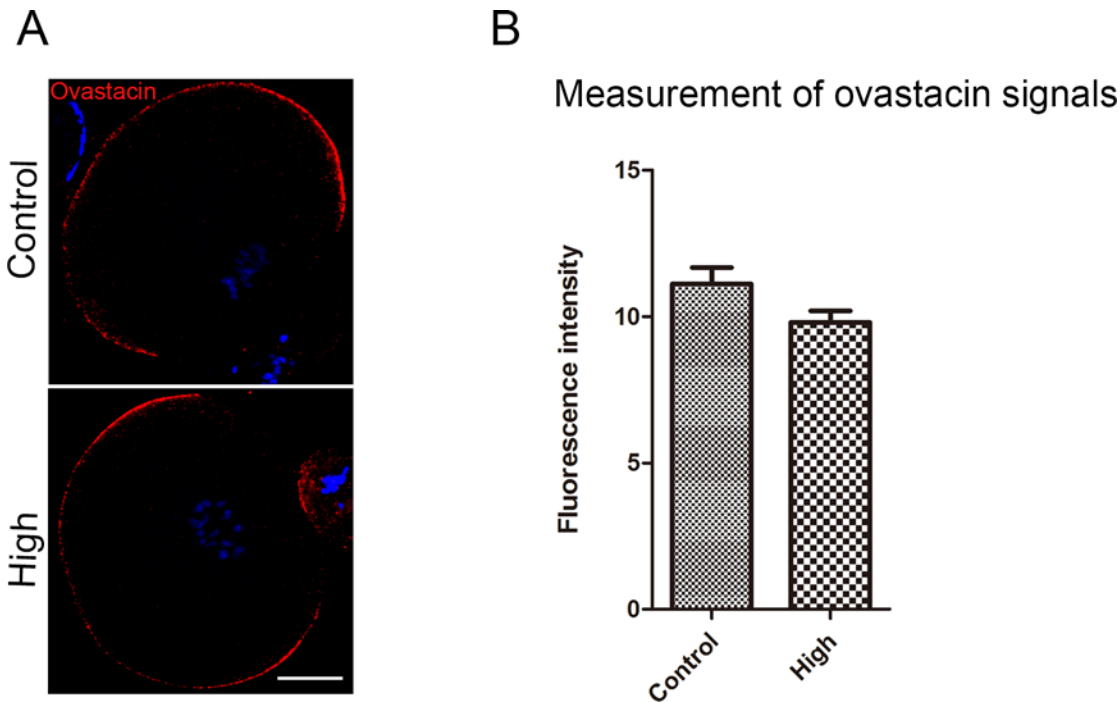


**Fig 2. Effect of melamine feeding on the ovastacin localization and protein level in ovulated eggs.** (A) Ovastacin was stained with rabbit polyclonal anti-mouse ovastacin antibody and examined by confocal microscopy. Scale bar, 20 $\mu$ m. (B) Measurement of fluorescent intensity of ovastacin signals. There was no significant difference of ovastacin signals between control (n = 15) and treatment (n = 15) groups. Data were presented as mean percentage (mean  $\pm$  SEM) of at least three independent experiments. Asterisk denotes statistical difference at a P < 0.05 level of significance.

doi:10.1371/journal.pone.0144248.g002

granules which is responsible for post-fertilization cleavage of N-terminus of ZP2, the sperm binding site in the zona pellucida, to block polyspermy, because mislocalization and premature release of ovastacin before fertilization in unfertilized eggs would lead to zona hardening so that compromise the fertilization. To validate this, we performed the immunostaining of ovastacin under the same condition in control and melamine fed groups, and measured the immunofluorescent intensity. As shown in Fig 2, ovastacin was localized under the oocyte subcortical region and excluded in cortical granule free domain, and both localization and signal intensity of ovastacin were comparable between control and high-dose groups (11.1  $\pm$  0.6% VS 9.9  $\pm$  0.4%), indicating that melamine would not lead to the mislocalization and premature exocytosis of ovastacin, which might be one of the factors leading to the fertilization failure.

### Melamine does not affect sperm binding ability on eggs

Next, we tested if melamine has effect on the sperm–zona pellucida binding *in vitro*. Based on the fact that sperm bind to the N-terminus of ZP2 in unfertilized eggs but not 2-cell embryos in which has been cleaved by ovastacin released by cortical granules, we set up 2-cell embryos as the negative control for the sperm binding assay. The immunofluorescent analysis showed that the number of sperm binding to the surface of zona pellucida surrounding eggs from both control and high-dose groups is comparable (94.0  $\pm$  3.5% VS 95.8  $\pm$  4.3%) (Fig 3A, 3B and 3C), suggesting that impairment of the fertilization capability of eggs by melamine does not result from the zona binding defect. Because sperm binding to zona is determined by the cleavage status of ZP2, we also performed the western blot using the antibody M2c.2 which recognizes the C-terminus of mouse ZP2. In the control group, ZP2 remained intact in unfertilized eggs and

cleaved in 2-cell embryos as expected (Fig 3D). In high-dose group, there was no ZP2 cleavage detected in unfertilized eggs, consistent with the above result that sperm binding ability is normal in melamine-treated eggs.

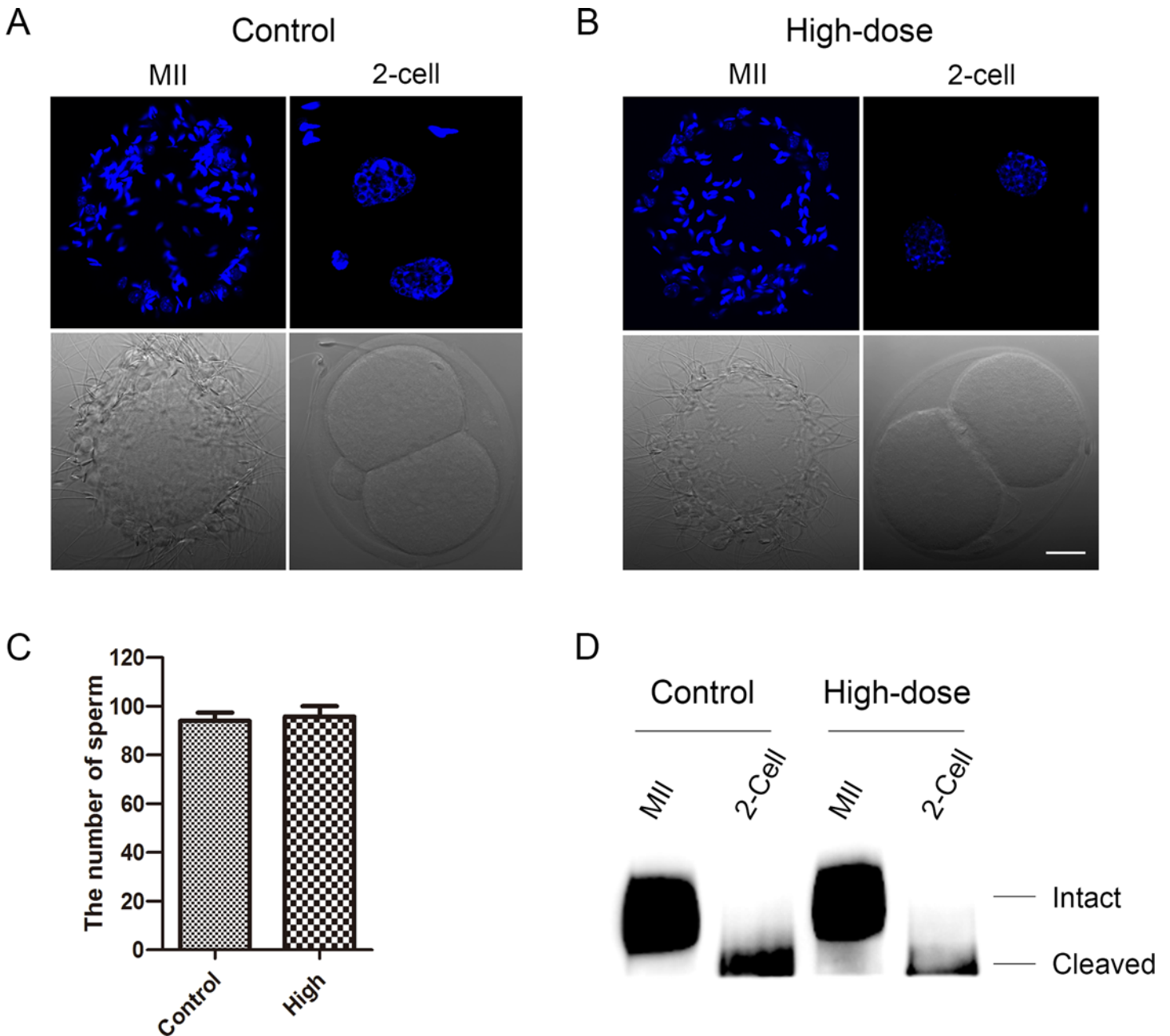


**Fig 3. Sperm binding capability and ZP2 cleavage status.** (A, B) Eggs and two-cell embryos from control and melamine fed mice were incubated with capacitated sperm for 1 hr. After washing with a wide-bore pipette to remove all but two to six sperm on normal two-cell embryos (negative control), eggs and embryos with sperm were fixed and stained with Hoechst 33342. Scale bar, 20 $\mu$ m. (C) The number of sperm binding to the surface of zona pellucida surrounding eggs. There was no significant difference between control (n = 10) and high-dose (n = 8) groups. (D) Western blot analysis of ZP2 cleavage status in eggs and two-cell embryos using M2c.2 antibody that recognizes the C-terminal domain of ZP2. The size of intact ZP2 is 120 kD, and the size of cleaved C-terminal fragment of ZP2 is 90 kD.

doi:10.1371/journal.pone.0144248.g003

### Melamine exposure reduces Juno protein level on the egg membrane

Since we have already ruled out the defect on the zona pellucida, we further explored the possible candidates on the egg membrane. Juno is a recently-found receptor on the egg membrane which binds to Izumo1 in the sperm head to mediate the sperm-egg fusion. We performed the immunostaining of Juno, and found that it was evenly distributed on the egg membranes (Fig 4A). Furthermore, we measured the immunofluorescent intensity of egg membranes in control and high-dose groups, and the result showed that the protein level of Juno in the high-dose group was remarkably lower than that in control group ( $11.6 \pm 0.3$  VS  $24.2 \pm 0.6$ ,  $P < 0.01$ , Fig 4B). Thus, the subfertility phenotype induced by melamine is probably caused by the decreased level of Juno on the egg membrane.

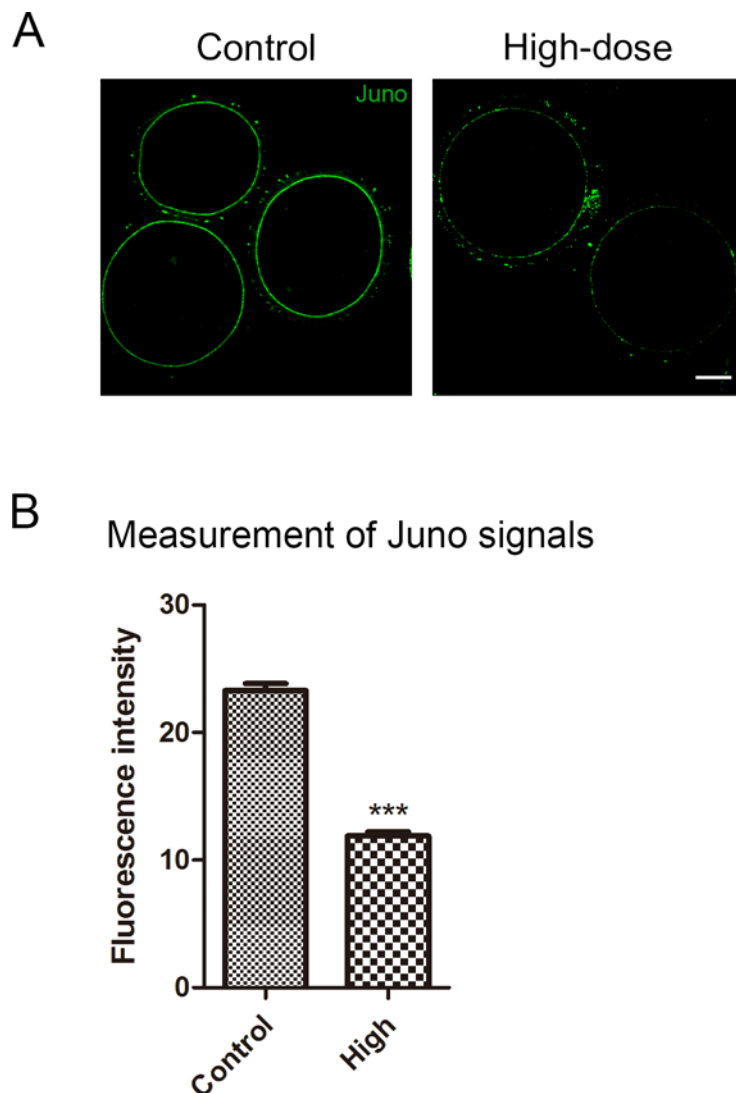


**Fig 4. Effect of melamine feeding on the protein level of Juno in ovulated eggs.** (A) Juno was stained with rat monoclonal anti-mouse folr4 antibody and examined by confocal microscopy. Scale bar, 20 $\mu$ m. (B) Measurement of fluorescent intensity of Juno signals. The protein level of Juno in egg membrane was significantly reduced in high-dose group (n = 15) compared to control group (n = 25). Data were presented as mean percentage (mean  $\pm$  SEM) of at least three independent experiments. Asterisk denotes statistical difference at a  $P < 0.05$  level of significance.

doi:10.1371/journal.pone.0144248.g004

## Discussion

Melamine (2, 4, 6-triamino-1, 3, 5-triazine), a chemical material, is a widely used industrial chemical that is not considered acutely toxic with a high LD<sub>50</sub> in animals, and the oral LD<sub>50</sub> ranges from 3.2 g/kg to 7.0 g/kg in mice [21]. However, long-term exposure to melamine could lead to infertility in rat males [4]. Also, our most recent report indicates that melamine negatively affects female fertility in mice [5].

In the present study, we further investigated the possible molecular mechanism regarding the effect of melamine on the fertility of female mice. We found that feeding mice with the melamine-contained diet had no effects on the ovastacin localization and exocytosis, as well as the sperm-zona pellucida binding, but indeed compromised the Juno protein level on the egg membrane, which might be the major cause leading to the female subfertility.

Fertilization is a unique and multi-step event that initiates the onset of development. During mammalian fertilization, capacitated sperm must bind to and penetrate the specialized extracellular matrix of the egg, known as zona pellucida, and then fuse with the oolemma to become the fertilized eggs [8]. The mouse genetic studies have defined the N-terminal domain of ZP2 as the sperm binding site in the zona pellucida, and the sperm binding is determined by the ZP2 cleavage status independent of fertilization [9]. Following fertilization, ZP2 undergoes proteolytic cleavage by an oocyte-specific astacin-like metalloendoprotease, first reported as ovastacin (citation), released from the cortical granules, and sperm no longer bind to mouse embryos [22]. However, if ovastacin is exocytosed during oogenesis or oocyte maturation before fertilization, it will prematurely cleave the N-terminus of ZP2 and result in less or no sperm binding, leading to the fertilization failure. Based on these understandings, we examined the possible reasons that would cause the melamine-induced female subfertility in mice one after another. Normal localization and protein level of ovastacin in melamine exposed eggs indicated that impairment of fertility is not due to the defect of ovastacin. Next, we tested the sperm binding to zona pellucida. Both sperm binding assay and western blot analysis of ZP2 cleavage revealed that melamine does not result in the zona defect.

Juno is an essential cell-surface protein as the receptor for Izumo1 on the plasma membrane of mouse eggs [7]. Juno and Izumo1 play crucial role in sperm-egg fusion in mice [7, 23, 24]. In other words, both Juno-deficient females and Izumo1-deficient males are infertile because their gametes cannot fuse to their wild-type partner's cells. Therefore, we aimed Juno as our next candidate. Our immunostaining and signal measurement results showed that high-dose (50mg/kg/d) feeding of melamine to female mice led to significant decrease of Juno protein level on the plasma membrane of unfertilized eggs. This finding consistently interprets the subfertility phenotype, because the small amount of remaining Juno renders some melamine-exposed eggs still fertilizable.

Taken together, we present data here to demonstrate that melamine negatively affects female fertility through suppressing Juno protein level in mice. As for how melamine regulates its protein expression or degradation, it needs the more in-depth investigation in the future.

## Acknowledgments

We thank Dr. Jurrien Dean very much for providing antibodies.

## Author Contributions

Conceived and designed the experiments: XXD SCS BX. Performed the experiments: XXD MQZ YJL YLM CYZ. Analyzed the data: XXD BX. Wrote the paper: XXD BX.

## References

1. Cook HA, Klampfl CW, Buchberger W. Analysis of melamine resins by capillary zone electrophoresis with electrospray ionization-mass spectrometric detection. *Electrophoresis*. 2005; 26(7–8):1576–83. doi: [10.1002/elps.200410058](https://doi.org/10.1002/elps.200410058) PMID: [15759307](https://pubmed.ncbi.nlm.nih.gov/15759307/).
2. Ingelfinger JR. Melamine and the global implications of food contamination. *The New England journal of medicine*. 2008; 359(26):2745–8. doi: [10.1056/NEJMp0808410](https://doi.org/10.1056/NEJMp0808410) PMID: [19109571](https://pubmed.ncbi.nlm.nih.gov/19109571/).
3. Hau AK, Kwan TH, Li PK. Melamine toxicity and the kidney. *Journal of the American Society of Nephrology: JASN*. 2009; 20(2):245–50. doi: [10.1681/ASN.2008101065](https://doi.org/10.1681/ASN.2008101065) PMID: [19193777](https://pubmed.ncbi.nlm.nih.gov/19193777/).
4. Bock M, Jackson H. The action of triethylenemelamine on the fertility of male rats. *British journal of pharmacology and chemotherapy*. 1957; 12(1):1–7. PMID: [13413142](https://pubmed.ncbi.nlm.nih.gov/13413142/); PubMed Central PMCID: PMC1509654.
5. Duan X, Dai XX, Wang T, Liu HL, Sun SC. Melamine negatively affects oocyte architecture, oocyte development and fertility in mice. *Human reproduction*. 2015; 30(7):1643–52. doi: [10.1093/humrep/dev091](https://doi.org/10.1093/humrep/dev091) PMID: [25924656](https://pubmed.ncbi.nlm.nih.gov/25924656/).
6. Bianchi E, Wright GJ. Izumo meets Juno: preventing polyspermy in fertilization. *Cell cycle*. 2014; 13(13):2019–20. doi: [10.4161/cc.29461](https://doi.org/10.4161/cc.29461) PMID: [24906131](https://pubmed.ncbi.nlm.nih.gov/24906131/); PubMed Central PMCID: PMC4111690.
7. Bianchi E, Doe B, Goulding D, Wright GJ. Juno is the egg Izumo receptor and is essential for mammalian fertilization. *Nature*. 2014; 508(7497):483–7. doi: [10.1038/nature13203](https://doi.org/10.1038/nature13203) PMID: [24739963](https://pubmed.ncbi.nlm.nih.gov/24739963/); PubMed Central PMCID: PMC3998876.
8. Wassarman PM, Jovine L, Litscher ES, Qi H, Williams Z. Egg-sperm interactions at fertilization in mammals. *European journal of obstetrics, gynecology, and reproductive biology*. 2004; 115 Suppl 1:S57–60. doi: [10.1016/j.ejogrb.2004.01.025](https://doi.org/10.1016/j.ejogrb.2004.01.025) PMID: [15196717](https://pubmed.ncbi.nlm.nih.gov/15196717/).
9. Avella MA, Xiong B, Dean J. The molecular basis of gamete recognition in mice and humans. *Molecular human reproduction*. 2013; 19(5):279–89. doi: [10.1093/molehr/gat004](https://doi.org/10.1093/molehr/gat004) PMID: [23335731](https://pubmed.ncbi.nlm.nih.gov/23335731/); PubMed Central PMCID: PMC3632220.
10. Wassarman PM. Mammalian fertilization: molecular aspects of gamete adhesion, exocytosis, and fusion. *Cell*. 1999; 96(2):175–83. PMID: [9988213](https://pubmed.ncbi.nlm.nih.gov/9988213/).
11. Wassarman PM, Jovine L, Litscher ES. A profile of fertilization in mammals. *Nature cell biology*. 2001; 3(2):E59–64. doi: [10.1038/35055178](https://doi.org/10.1038/35055178) PMID: [11175768](https://pubmed.ncbi.nlm.nih.gov/11175768/).
12. Gupta SK, Bhandari B, Shrestha A, Biswal BK, Palaniappan C, Malhotra SS, et al. Mammalian zona pellucida glycoproteins: structure and function during fertilization. *Cell and tissue research*. 2012; 349(3):665–78. doi: [10.1007/s00441-011-1319-y](https://doi.org/10.1007/s00441-011-1319-y) PMID: [22298023](https://pubmed.ncbi.nlm.nih.gov/22298023/).
13. Clark GF. The molecular basis of mouse sperm-zona pellucida binding: a still unresolved issue in developmental biology. *Reproduction*. 2011; 142(3):377–81. doi: [10.1530/REP-11-0118](https://doi.org/10.1530/REP-11-0118) PMID: [21730109](https://pubmed.ncbi.nlm.nih.gov/21730109/).
14. Burkart AD, Xiong B, Baibakov B, Jimenez-Movilla M, Dean J. Ovastacin, a cortical granule protease, cleaves ZP2 in the zona pellucida to prevent polyspermy. *The Journal of cell biology*. 2012; 197(1):37–44. doi: [10.1083/jcb.201112094](https://doi.org/10.1083/jcb.201112094) PMID: [22472438](https://pubmed.ncbi.nlm.nih.gov/22472438/); PubMed Central PMCID: PMC3317803.
15. Bond JS, Beynon RJ. The astacin family of metalloendopeptidases. *Protein science: a publication of the Protein Society*. 1995; 4(7):1247–61. doi: [10.1002/pro.5560040701](https://doi.org/10.1002/pro.5560040701) PMID: [7670368](https://pubmed.ncbi.nlm.nih.gov/7670368/); PubMed Central PMCID: PMC2143163.
16. Dumermuth E, Sterchi EE, Jiang WP, Wolz RL, Bond JS, Flannery AV, et al. The astacin family of metalloendopeptidases. *The Journal of biological chemistry*. 1991; 266(32):21381–5. PMID: [1939172](https://pubmed.ncbi.nlm.nih.gov/1939172/).
17. Dietzel E, Wessling J, Floehr J, Schafer C, Ensslen S, Denecke B, et al. Fetuin-B, a liver-derived plasma protein is essential for fertilization. *Developmental cell*. 2013; 25(1):106–12. doi: [10.1016/j.devcel.2013.03.001](https://doi.org/10.1016/j.devcel.2013.03.001) PMID: [23562279](https://pubmed.ncbi.nlm.nih.gov/23562279/).
18. Stocker W, Karmilin K, Hildebrand A, Westphal H, Yiallourous I, Weiskirchen R, et al. Mammalian gamete fusion depends on the inhibition of ovastacin by fetuin-B. *Biological chemistry*. 2014; 395(10):1195–9. doi: [10.1515/hsz-2014-0189](https://doi.org/10.1515/hsz-2014-0189) PMID: [25205729](https://pubmed.ncbi.nlm.nih.gov/25205729/).
19. Alfieri JA, Martin AD, Takeda J, Kondoh G, Myles DG, Primakoff P. Infertility in female mice with an oocyte-specific knockout of GPI-anchored proteins. *Journal of cell science*. 2003; 116(Pt 11):2149–55. doi: [10.1242/jcs.00430](https://doi.org/10.1242/jcs.00430) PMID: [12692150](https://pubmed.ncbi.nlm.nih.gov/12692150/).
20. Coonrod SA, Naaby-Hansen S, Shetty J, Shibahara H, Chen M, White JM, et al. Treatment of mouse oocytes with PI-PLC releases 70-kDa (pI 5) and 35- to 45-kDa (pI 5.5) protein clusters from the egg surface and inhibits sperm-oolemma binding and fusion. *Developmental biology*. 1999; 207(2):334–49. doi: [10.1006/dbio.1998.9161](https://doi.org/10.1006/dbio.1998.9161) PMID: [10068467](https://pubmed.ncbi.nlm.nih.gov/10068467/).
21. Skinner CG, Thomas JD, Osterloh JD. Melamine toxicity. *Journal of medical toxicology: official journal of the American College of Medical Toxicology*. 2010; 6(1):50–5. doi: [10.1007/s13181-010-0038-1](https://doi.org/10.1007/s13181-010-0038-1) PMID: [20195812](https://pubmed.ncbi.nlm.nih.gov/20195812/); PubMed Central PMCID: PMC3550444.

22. Bleil JD, Beall CF, Wassarman PM. Mammalian sperm-egg interaction: fertilization of mouse eggs triggers modification of the major zona pellucida glycoprotein, ZP2. *Developmental biology*. 1981; 86(1):189–97. PMID: [6793422](#).
23. Ohnami N, Nakamura A, Miyado M, Sato M, Kawano N, Yoshida K, et al. CD81 and CD9 work independently as extracellular components upon fusion of sperm and oocyte. *Biology open*. 2012; 1(7):640–7. doi: [10.1242/bio.20121420](#) PMID: [23213457](#); PubMed Central PMCID: PMC3507294.
24. Inoue N, Ikawa M, Isotani A, Okabe M. The immunoglobulin superfamily protein Izumo is required for sperm to fuse with eggs. *Nature*. 2005; 434(7030):234–8. doi: [10.1038/nature03362](#) PMID: [15759005](#).



项目批准号	31571545
申请代码	C120202
归口管理部门	
依托单位代码	21009508A1649-1247



# 国家自然科学基金委员会 资助项目计划书

资助类别：面上项目

亚类说明：

附注说明：常规面上项目

项目名称：利用Ovastacin-mCherry转基因小鼠研究哺乳动物皮质颗粒的动态转运及调控机理

直接费用：60万元                      间接费用：11.6万元

项目资金：71.6万元                      执行年限：2016.01-2019.12

负责人：熊波

通讯地址：南京农业大学动物科技学院

邮政编码：                                      电      话：025-84399605

电子邮件：xiongbo@njau.edu.cn

依托单位：南京农业大学

联系人：张红霞                                      电      话：025-84395725

填表日期：                                      2015年08月21日



## 国家自然科学基金委员会资助项目计划书填报说明

- 一、项目负责人收到《关于国家自然科学基金资助项目批准及有关事项的通知》（以下简称《批准通知》）后，请认真阅读本填报说明，参照国家自然科学基金相关项目管理办法及《国家自然科学基金资助项目资金管理办法》（请查阅国家自然科学基金委员会官方网站首页“政策法规”-“管理办法”栏目），按《批准通知》的要求认真填写和提交《国家自然科学基金委员会资助项目计划书》（以下简称《计划书》）。
- 二、填写《计划书》时要求科学严谨、实事求是、表述清晰、准确。《计划书》经国家自然科学基金委员会相关项目管理部门审核批准后，将作为项目研究计划执行和检查、验收的依据。
- 三、《计划书》各部分填写要求如下：
  - （一）简表：由系统自动生成。
  - （二）摘要及关键词：各类获资助项目都必须填写中、英文摘要及关键词。
  - （三）项目组主要成员：计划书中列出姓名的项目组主要成员由系统自动生成，与申请书原成员保持一致，不可随意调整。如果批准通知中“项目评审意见及修改意见表”中“对研究方案的修改意见”栏目有调整项目组成员相关要求的，待项目开始执行后，按照项目成员变更程序另行办理。
  - （四）资金预算表：按批准资助的直接费用填报资金预算表和预算说明书，其中的劳务费、专家咨询费金额不应高于申请书中相应金额；间接费用及项目总经费由系统自动生成。国家重大科研仪器研制项目还应按照预算评审后批复的直接费用各科目金额填报资金预算表、预算说明书及相应的预算明细表。
  - （五）正文：
    1. 面上项目、青年科学基金项目、地区科学基金项目：如果《批准通知》中没有修改要求的，只需选择“研究内容和研究目标按照申请书执行”即可；如果《批准通知》中“项目评审意见及修改意见表”中“对研究方案的修改意见”栏目明确要求调整研究期限和研究内容等的，须选择“根据研究方案修改意见更改”并填报相关修改内容。
    2. 重点项目、重点国际（地区）合作研究项目、重大项目、国家重大科研仪器研制项目：须选择“根据研究方案修改意见更改”，根据《批准通知》的要求填写研究（研制）内容，不得自行降低、更改研究目标（或仪器研制的技术性能与主要技术指标以及验收技术指标）或缩减研究（研制）内容。此外，还要突出以下几点：
      - （1）研究的难点和在实施过程中可能遇到的问题（或仪器研制风险），拟采用的研究（研制）方案和技术路线；
      - （2）项目主要参与者分工，合作研究单位之间的关系与分工，重大项目还需说明课题之间的关联；
      - （3）详细的年度研究（研制）计划。



3. 国家杰出青年科学基金、优秀青年科学基金和海外及港澳学者合作研究基金项目：须选择“根据研究方案修改意见更改”，按下列提纲撰写：
  - (1) 研究方向；
  - (2) 结合国内外研究现状，说明研究工作的学术思想和科学意义（限两个页面）；
  - (3) 研究内容、研究方案及预期目标（限两个页面）；
  - (4) 年度研究计划；
  - (5) 研究队伍的组成情况。
4. 对于其他类型项目，参照面上项目的方式进行选择和填写。



## 简表

申请者信息	姓名	熊波	性别	男	出生年月	1980年05月	民族	汉族	
	学位	博士			职称	教授			
	电话	025-84399605		电子邮件	xiongbo@njau.edu.cn				
	传真			个人网页					
	工作单位	南京农业大学							
	所在院系所	动物科技学院							
依托单位信息	名称	南京农业大学					代码	21009508A1649	
	联系人	张红霞		电子邮件	kjcxm@njau.edu.cn				
	电话	025-84395725		网站地址	http://www.njau.edu.cn				
合作单位信息	单位名称							代码	
项目基本信息	项目名称	利用Ovastacin-mCherry转基因小鼠研究哺乳动物皮质颗粒的动态转运及调控机理							
	资助类别	面上项目			亚类说明				
	附注说明	常规面上项目							
	申请代码	C120202:卵巢功能与卵子成熟							
	基地类别	23269002. 动物生理生化实验室							
	执行年限	2016.01-2019.12							
	直接费用	60万元			间接费用	11.6万元			
	项目资金	71.6万元							



## 项目摘要

### 中文摘要(500字以内):

多精受精是指超过一个精子进入卵子形成多个原核的异常受精形式,最终会导致早期胚胎死亡。卵子防止多精受精的机制主要与一种被称为皮质颗粒的特殊细胞器有关,它是存在于未受精卵母细胞皮质区的一层分泌囊泡。受精后,皮质颗粒释放其内容物至卵周隙,修饰细胞外基质以阻止多精受精。目前有关皮质颗粒成分和功能的认识主要来自于海胆等无脊椎动物,对哺乳动物的皮质颗粒知之甚少。最近,在小鼠中Ovastacin首次被鉴定为哺乳动物的皮质颗粒成分,负责受精后切割卵透明带中的精子受体ZP2来防止多精受精。本项目将利用Ovastacin作为皮质颗粒的标识物,构建Ovastacin-mCherry转基因小鼠,探索皮质颗粒在卵子成熟和受精中的转运及调控机制,阐明皮质颗粒转运和释放异常导致受精失败和引起多精受精的根本原因,并分离鉴定皮质颗粒的其它未知成分和功能,为全面了解哺乳动物皮质颗粒在生殖生物学和生殖医学中的意义提供研究基础。

**关键词:** 小鼠; 卵母细胞; 卵子成熟; 减数分裂; 卵子质量

### Abstract(limited to 4000 words):

Polyspermy, an abnormal fertilization, forms multiple pronuclei by allowing more than one sperm entry into the eggs, which would cause early embryonic lethality. The block to polyspermy is related to a unique organelle called cortical granules located in the cortex of unfertilized oocytes. Following fertilization, cortical granules undergo exocytosis to release their contents into the perivitelline space, and then modify the extracellular matrix to prevent polyspermy. The previous studies on the cortical granules mainly originate from invertebrates such as sea urchin, little is known about contents and functions of mammalian cortical granules. Not till recently, Ovastacin has been firstly identified as one of the components of cortical granules in the mouse. Thus, the present project will establish an Ovastacin-mCherry transgenic mouse model, taking advantage of Ovastacin as the marker of cortical granules to investigate its dynamic trafficking and regulatory mechanisms during mouse oocyte maturation and fertilization, explicating the molecular basis regarding the fertilization failure and polyspermy caused by the aberrant translocation and exocytosis of cortical granules. Also, density gradient centrifugation coupled with fluorescence-activated cell sorting will be used to isolate and identify more contents of cortical granules to discover their extra functions in the reproduction, providing fundamental basis to learn the significance of mammalian cortical granules in the reproductive biology and medicine.

**Keywords:** Mouse; Oocyte; Oocyte maturation; Meiosis; Oocyte quality



## 项目组主要成员

编号	姓名	出生年月	性别	职称	学位	单位名称	电话	证件号码	项目分工	每年工作时间(月)			
1	熊波	1980.05	男	教授	博士	南京农业大学	025-84399605	360102198005295810	项目负责人	10			
2	侯艳君	1985.10	女	博士后	博士	南京农业大学	025-84399605	410603198510121529	皮质颗粒的分离与鉴定	10			
3	代小新	1988.01	女	博士生	硕士	南京农业大学	025-84399605	372923198801012921	显微注射、小鼠模型构建等	10			
4	张冕群	1991.02	女	硕士生	学士	南京农业大学	025-84399605	341002199102129429	载体构建、活细胞观察等	10			
总人数		高级		中级		初级		博士后		博士生		硕士生	
4		1						1		1		1	



## 国家自然科学基金项目资金预算表（定额补助）

项目名称：利用Ovastacin-mCherry转基因小鼠研究哺乳动物皮质颗粒的动态转运及调控机理

项目负责人：熊波

金额单位：万元

序号	科目名称	金额	备注
	(1)	(2)	(3)
1	一、项目资金支出	71.6000	/
2	(一) 直接费用	60.0000	
3	1、设备费	2.0000	
4	(1) 设备购置费	2.0000	购买一台计算机和一台小型离心机
5	(2) 设备试制费	0.0000	
6	(3) 设备改造与租赁费	0.0000	
7	2、材料费	34.0000	生化试剂、抗体、实验动物、培养试剂等
8	3、测试化验加工费	4.0000	激光共聚焦、活细胞工作站等设备使用费
9	4、燃料动力费	0.0000	
10	5、差旅费	3.0000	参加国内学术会议注册费、差旅费
11	6、会议费	0.0000	
12	7、国际合作与交流费	4.0000	参加国际学术会议费用
13	8、出版/文献/信息传播/知识产权事务费	3.0000	发表SCI论文版面费、彩图费
14	9、劳务费	10.0000	直接参加项目的研究生劳务费
15	10、专家咨询费	0.0000	
16	11、其他支出	0.0000	
17	(二) 间接费用	11.6000	管理费、绩效支出等
18	其中：绩效支出	2.9000	绩效支出
19	二、自筹资金	0.0000	



## 预算说明书

(请对各项支出的主要用途和测算理由及合作研究外拨资金等内容进行详细说明, 可根据需要另加附页。)

- 1) 设备费2万元, 购买一台计算机约5000元用于数据分析, 一台小型离心机约15000元供分子生物学实验用。
- 2) 材料费34万元, 包括: 实验小鼠的繁殖和饲养费用4年约为100000元(学校收费为每只每日1元, 按平均100只算), 利用Crispr/Cas9制作小鼠模型约80000元(小鼠模型制作成本高), 小鼠基因型鉴定所需试剂和试剂盒20000元(小鼠尾巴裂解液, Tag酶, DNA提取试剂盒等), 4年所需抗体约10支30000元(不同目的蛋白抗体以及各种marker级抗体), 制作用于显微注射的mRNA和sgRNA所需的载体、限制性内切酶等分子克隆试剂和各种试剂盒约40000元, 4年所需基因测序和引物合成费用20000元, 小鼠卵母细胞培养试剂和一次性消耗器材如培养皿等约50000元。
- 3) 测试费、差旅费共7万元, 包括: 大型公用仪器如激光共聚焦显微镜、活细胞工作站等使用费(学校内部使用费40元, 由于活细胞工作站需要长时间连续观察, 每年大约需要使用250小时, 4年费用为 $40 \times 250 \times 4 = 40000$ 元)。带领一至两名学生参加三次国内会议, 所需注册费10000元、差旅费20000元, 共30000元。
- 4) 国际合作费、出版费共7万元。发表3篇SCI论文所需的彩图费和版面费约30000元(每篇SCI论文版面和彩图费平均约为1500美元)。国际交流合作费约4万元, 包括参加两次国际学术会议展示研究成果: 一次美国生殖生物学年会SSR, 一次亚洲繁殖生物技术大会ARBS, 两次合计40000元。
- 5) 剩余费用为支付劳务费10万元(3名研究生4年每个月800元补助,  $3 \times 4 \times 10 \times 800 \approx 100000$ 元)和自动生成的间接费用11.6万元。

项目负责人签字:

科研部门公章:

财务部门公章:



## 报告正文

研究内容和研究目标按照申请书执行。



## 国家自然科学基金资助项目签批审核表

<p>我接受国家自然科学基金的资助，将按照申请书、项目批准意见和计划书负责实施本项目（批准号：31571545），严格遵守国家自然科学基金委员会关于资助项目管理、财务等各项规定，切实保证研究工作时间，认真开展研究工作，按时报送有关材料，及时报告重大情况变动，对资助项目发表的论著和取得的研究成果按规定进行标注。</p> <p style="text-align: right; margin-top: 20px;">项目负责人（签章）： 年 月 日</p>	<p>我单位同意承担上述国家自然科学基金项目，将保证项目负责人及其研究队伍的稳定和研究项目实施所需的条件，严格遵守国家自然科学基金委员会有关资助项目管理、财务等各项规定，并督促实施。</p> <p style="text-align: right; margin-top: 20px;">依托单位（公章） 年 月 日</p>																				
本 栏 目 由 基 金 委 填 写	科学处审查意见：																				
	建议年度拨款计划（本栏目为自动生成，单位：万元）：																				
	<table border="1" style="width: 100%; border-collapse: collapse; text-align: center;"> <thead> <tr> <th style="width: 10%;">年度</th> <th style="width: 10%;">总额</th> <th style="width: 10%;">第一年</th> <th style="width: 10%;">第二年</th> <th style="width: 10%;">第三年</th> <th style="width: 10%;">第四年</th> <th style="width: 10%;">第五年</th> </tr> </thead> <tbody> <tr> <td>金额</td> <td></td> <td></td> <td></td> <td></td> <td></td> <td></td> </tr> </tbody> </table>	年度	总额	第一年	第二年	第三年	第四年	第五年	金额												
年度	总额	第一年	第二年	第三年	第四年	第五年															
金额																					
科学部审查意见：							负责人（签章）： 年 月 日														
本 栏 目 主 要 用 于 重 大 项 目 等	相关局室审核意见：							负责人（签章）： 年 月 日													
	委领导审批意见：							委领导（签章）： 年 月 日													

# 江苏省科技项目合同

计划类别 基础研究计划（自然科学基金）--青年基金项目

项目编号 BK20150677

项目名称 哺乳动物皮质颗粒动态转运影响受精的机制研究

项目类别 \_\_\_\_\_

起止年限 2015 年 7 月至 2018 年 6 月

项目负责人 熊波 电话及手机 15850502046 025-84399605

\_\_\_\_\_ 电话及手机 \_\_\_\_\_

承担单位 南京农业大学

单位地址 南京市玄武区卫岗1号 邮政编码 210095

项目主管部门 南京农业大学

江苏省科学技术厅

二〇一五年

**委托单位（甲方）：** 江苏省科学技术厅

法定代表人： 王秦

地址： 南京市北京东路 39 号

邮政编码： 210008

**承担单位（乙方）：**

承担单位： 南京农业大学

法定代表人： 周光宏

地址： 南京市玄武区卫岗 1 号 邮政编码： 210095

项目负责人： 熊波

电话： 15850502046 传真：         

电子邮件： kjcxmk@njau.edu.cn

**保证单位（丙方、项目主管部门）：** 南京农业大学

法定代表人（科技局局长）：         

地址：          邮政编码：         

甲方批准由乙方承担省科技计划《哺乳动物皮质颗粒动态转运影响受精的机制研究》项目的研究开发或建设任务。依据《中华人民共和国合同法》的规定，为明确甲、乙、丙三方的权利和责任，保证项目的顺利实施和科研经费的合理使用，签订本合同。

## 一、项目的目标和主要研究内容

要解决的主要技术难题和问题，项目研究的创新点和内容等。

- 1、利用微丝和微管的解聚剂，以及微丝成核因子和微管动力蛋白的抑制剂处理 Ovastacin-mCherry 转基因小鼠的卵母细胞，观察卵母细胞成熟过程中 mCherry 从胞质向皮质区的转运。
- 2、采用荧光漂白恢复术淬灭 Ovastacin-mCherry 在皮质区的荧光信号，实时记录信号的恢复情况，确定皮质颗粒在皮质区的定位是否是动态变化的。
- 3、利用细胞骨架解聚剂研究无皮质颗粒区的形成机制。
- 4、实时观察卵子受精后排放皮质颗粒的过程，确定皮质颗粒排放与卵子质膜及透明带对精子接受性的时空关系，以及实时记录卵子老化过程中皮质颗粒的动态变化，确定老化卵子中皮质颗粒提前释放与受精率下降的关系。

江苏省科学技术厅

## 二、项目验收内容和考核指标

包括 1、主要技术指标：如形成的专利、新技术、新产品、新装置、论文专著等数量、指标及其水平等；2、主要经济指标：如技术及产品所形成的市场规模、效益等；3、项目实施中形成的示范基地、中试线、生产线及其规模等；4、其他应考核的指标。

利用微丝和微管的解聚剂，以及微丝成核因子和微管动力蛋白的抑制剂处理 Ovastacin-mCherry 转基因小鼠的卵母细胞，观察卵母细胞成熟过程中 mCherry 从胞质向皮质区的转运。采用荧光漂白恢复术淬灭 Ovastacin-mCherry 在皮质区的荧光信号，实时记录信号的恢复情况，确定皮质颗粒在皮质区的定位是否是动态变化的。利用细胞骨架解聚剂研究无皮质颗粒区的形成机制。实时观察卵子受精后排放皮质颗粒的过程，确定皮质颗粒排放与卵子质膜及透明带对精子接受性的时空关系，以及实时记录卵子老化过程中皮质颗粒的动态变化，确定老化卵子中皮质颗粒提前释放与受精率下降的关系。1、明确哺乳动物皮质颗粒在保证成功受精和防止多精受精中的具体作用和调控机理。2、利用皮质颗粒作为衡量卵子质量的标准，设计和开发卵子质量评估试剂盒。3、在生殖生物学领域的国际知名期刊发表 SCI 学术论文 2-3 篇。4、推动和改善体外受精技术以及冷冻卵子技术。5、参加国际会议展示相关研究成果。6、培养研究生 2-3 名。

江苏省科学技术厅

### 三、项目进度及考核指标

时 间	考核指标
2015年7月至2016年6月	繁殖 Ovastacin-mCherry 转基因小鼠，确定 Ovastacin-mCherry 转基因的功能性；以活细胞成像平台为基础，利用细胞骨架抑制剂深入探究皮质颗粒的转运和释放过程及机制，以及对受精或多精受精的影响；
2016年7月至2017年6月	采用荧光漂白恢复术确定皮质颗粒在皮质区的动态变化。利用微丝、微管解聚剂，以及脂类运动抑制剂确认影响其动态定位的因素；利用显微注射结合活细胞成像探明无皮质颗粒区形成的分子基础以及在受精过程中所起的作用。
2017年7月至2018年6月	实时观察卵子受精后排放皮质颗粒的过程，确定皮质颗粒排放与卵子质膜及透明带对精子接受性的时空关系。同时观察皮质颗粒排放被抑制后卵子质膜及透明带对精子的接受性；实时记录卵子老化过程中皮质颗粒的动态变化，确定老化卵子中皮质颗粒提前释放与受精率下降的关系；撰写论文并投稿。



## 五、项目经费预算

### (一) 项目经费来源预算

经费单位：万元

	合计	2015 年	2016 年	2017 年	备注
合计	20				
1、省拨款	20	20	0		
2、部门、地方配套	0				
3、承担单位自筹	0				
4、其他来源	0				

### (二) 项目经费支出预算

经费单位：万元

	预算数	其中：省拨款	备注
(一) 直接费用	17	17	
1、设备费	1	1	
(1) 购置设备费	1	1	购买一台计算机和一台数码相机
(2) 试制设备费	0	0	
(3) 设备改造与租赁费	0	0	
2、材料费	8	8	生化试剂、抗体、实验动物、培养试剂等
3、测试化验加工费	2	2	激光共聚焦、活细胞工作站等设备使用费
4、燃料动力费	0	0	
5、差旅费	2	2	参加国内学术会议注册费、差旅费
6、会议费	0	0	
7、国际合作与交流费	0	0	
8、出版/文献/信息传播/知识产权事务费	2	2	发表 SCI 论文版面费、彩图费
9、劳务费	2	2	直接参与项目的研究生劳务费

10、专家咨询费	0	0	
11、其他支出	0	0	
(二) 间接费用	3	3	管理费、绩效支出等
其中：绩效支出	0.8	0.8	绩效支出
合计	20	20	

## 六、其他条款

### (一) 缔约各方的权利、义务

第一条 缔约各方均应共同遵守国家、省有关科技计划与经费管理的规定，严格遵守并认真履行本合同的各项条款。

甲方应按合同约定的金额提供项目研究开发经费，有权监督、检查合同履行情况。合同履行期间，甲方有权直接组织或委托丙方检查、监督乙方对本合同的履行情况。乙方完成项目研究开发任务后，由甲方负责进行验收。

乙方应严格履行合同义务，为项目实施提供承诺的技术与条件保障，以及财务管理、成果管理、科技档案管理服务合同约定的其他义务。项目申请验收前乙方应按照规定提交科技报告，未提交科技报告的项目不予验收。乙方应加强项目实施成果的转化，自项目验收后一年内未实施转化的项目，甲方有权责成乙方将成果交省内技术产权交易机构挂牌转让。

丙方应按合同约定的金额提供项目配套经费，并进行相关的协调和监督。

第二条 甲方有权根据乙方项目计划进度完成情况决定是否拨付后续经费。乙方使用项目经费应按照合同约定的支出范围执行，保证专款专用，并实行单独核算，严禁弄虚作假、截留和挪用项目经费等违反财经纪律的行为。

第三条 甲、乙、丙各方对项目合同及其他技术资料负有保密责任。

### (二) 违约责任

第四条 甲方未能按合同约定的经费数提供经费，导致乙方研究开发工作延误的，应允许合同规定的研究开发工作完成期限相应顺延。

第五条 因乙方原因，导致研究开发工作未能达到合同约定指标的，乙方应采取措施尽快使项目达到合同预定要求，并承担由此而增加的费用。

第六条 乙方无正当理由未履行合同时，甲方有权停拨、追缴部分或全部省拨经费，由此造成的经济损失由乙方承担。对乙方在申报和实施项目中的失信行为，甲方将根据省科技信用管理的有关规定记入不良信用记录，并报送至省公共信用信息平台，列入乙方的社会信用记录。

第七条 乙方违反经费使用规定或经甲方检查确认计划进度不符合合同约定的，甲方有权减拨或停拨后续经费；情节严重的，甲方有权终止合同，乙方应返还甲方已拨付的全部经费。

第八条 乙方因不可抗力不能履行合同义务时，可以免除违约责任，但应及时通知甲、丙方，并在合理的期限内出具因不可抗力导致合同不能履行的证明。

第九条 在履行本合同过程中，确因在现有水平和条件下难以克服的技术困难，导致研究开发部分或全部失败造成损失的，经甲方确认风险责任后，甲方在其拨款额度范围内承担损失。

### （三）合同的变更、解除和争议解决

第十条 合同的变更或解除，须经缔约各方协商一致，并签署书面文件。

第十一条 发生下列情况之一的，缔约方应当协商变更或解除合同：

（1）由于不可抗力或意外事故导致合同无法履行或部分无法履行；

（2）由于项目目标已被他人先行实现，有关成果已被申请专利或公开，继续履行合同已无必要；

（3）由于乙方未按合同要求履行合同，或是由于其他原因，导致项目在检查或评估中被淘汰的。

第十二条 合同一方发生合并、分立或更名时，由变更后的单位继受或分别继受变更一方在合同中的权利义务。

第十三条 合同在履行过程中发生争议的，缔约各方应通过友好协商的方式解决。如协商不成时，缔约各方有权向人民法院起诉或仲裁机构申请仲裁，但在有关司法、仲裁结果生效之前，乙方有义务按照甲方要求继续履行或终止履行本合同。

### （四）附 则

第十四条 项目任务书、可行性论证报告作为合同附件。项目如涉及多家（包含两家）单位参加，乙方应在签订本合同前与有关单位就合作任务和知识产权分配等问题签订有关合同或协议（仅委托其他单位进行常规试验、提供社会化科技服务和少量辅助科研工作的情況除外），同时作为本合同的附件。

第十五条 有关合同的未尽事宜，按照国家、省有关科技计划与经费管理的规定执行。

第十六条 本合同正本一式六份（甲、乙、丙方各执2份），自缔约各方签章后生效。

第十七条 本合同的解释权归甲方享有。

## 七、附加条款

第十八条 省自然科学基金青年基金项目负责人在申报该类项目前，必须是未主持承担过省级或国家级科技计划项目（含国家自然科学基金项目）。否则，一经发现，按弄虚作假处理，取消该项目立项，并追究项目负责人、承担单位和科技主管部门责任。



江苏省科学技术厅

## 八、签订合同各方

甲方：

法定代表人或委托代理人（签字）

项目主管处室负责人（签字）

项目主管处室经办人（签字）

公 章

年 月 日

乙方：

承担单位法定代表人或委托代理人（签字）

项目负责人（签字）

开户银行、帐号

公 章

年 月 日

丙方：

法定代表人或委托代理人（签字）

公 章

年 月 日

**说明：**

1、本合同适用于省基础研究、科技支撑、科技基础设施、苏北发展、国际科技合作、软科学研究等计划。

2、合同条款中所有空项都需如实填写，确无此项的，请在该栏中打“/”或在空白处写“无”。

3、乙方盖章必须是单位公章，部门章无效。



江苏省科学技术厅